

UC Berkeley

UC Berkeley Previously Published Works

Title

Contribution of NK cells to immunotherapy mediated by PD-1/PD-L1 blockade

Permalink

<https://escholarship.org/uc/item/440969x8>

Journal

Journal of Clinical Investigation, 128(10)

ISSN

0021-9738

Authors

Hsu, Joy
Hodgins, Jonathan J
Marathe, Malvika
[et al.](#)

Publication Date

2018-10-01

DOI

10.1172/jci99317

Peer reviewed

1 **Title page:**

2 **Contribution of NK cells to immunotherapy mediated by PD-1/PD-L1 blockade.**

3
4 Joy Hsu^{1,†}, Jonathan J. Hodgins^{2,3,†}, Malvika Marathe¹, Chris J. Nicolai¹, Marie-Claude Bourgeois-
5 Daigneault^{2,3}, Troy N. Trevino¹, Camillia S. Azimi¹, Amit K. Scheer^{2,3}, Haley E. Randolph¹,
6 Thornton W. Thompson¹, Lily Zhang¹, Alexandre Iannello¹, Nikhita Mathur^{2,3}, Karen E. Jardine^{2,3},
7 Georgia A. Kim¹, John C. Bell^{2,3}, Michael W. McBurney^{2,3}, David H. Raulet^{1,*} Michele Ardolino^{1,2,3,*}

8
9 1: Department of Molecular and Cell Biology, Immunotherapy and Vaccine Research Initiative,
10 Cancer Research Laboratory, Division of Immunology and Pathogenesis, University of California,
11 Berkeley, Berkeley, CA, 94720, USA.

12 2: Department of Biochemistry, Microbiology and Immunology, University of Ottawa, Ottawa, ON
13 K1H 8M5, Canada

14 3: Centre for Cancer Therapeutics, Ottawa Hospital Research Institute, Ottawa, ON K1H 8L6,
15 Canada

16
17 †: JH and JJH equally contributed to this study.

18 *: DHR and MA equally contributed to this study.

19
20 correspondence to:

21 raulet@berkeley.edu

22 tel: 510-642-9521

23 485 LSA, Berkeley, CA, 94720-3200

24 and

25 m.ardolino@uottawa.ca

26 tel: 613-737-8899 x 77257

27 501 Smyth Road, Cancer Center, 3-328, Ottawa, ON, K1H8M2

28

29

30 Conflict of interest statement:

31 DHR is a co-founder of Dragonfly Therapeutics, and served on the Scientific Advisory Boards of
32 Innate Pharma, Aduro Biotech and Ignite Immunotherapy; he has a financial interest in all four
33 companies and received research support from Innate Pharma. JCB is a co-founder and have
34 equity in Turnstone Biologics from whom he receives a consulting fees and research support for
35 his lab. MCB and JCB have both patented intellectual properties, not related to the present
36 article.

37

38

39

40

41 **Abstract:**

42 Checkpoint blockade immunotherapy targeting the PD-1/PD-L1 inhibitory axis has produced
43 remarkable results in the treatment of several types of cancer. Whereas cytotoxic T cells are
44 known to provide important anti-tumor effects during checkpoint blockade, certain cancers with low
45 MHC expression are responsive to therapy, suggesting that other immune cell types may also play
46 a role. Here, we employed several mouse models of cancer to investigate the effect of PD-1/PD-L1
47 blockade on natural killer (NK) cells, a population of cytotoxic innate lymphocytes that also mediate
48 anti-tumor immunity. We discovered that PD-1 and PD-L1 blockade elicited a strong NK cell
49 response that was indispensable for the therapeutic effect of immunotherapy. PD-1 was expressed
50 on NK cells within transplantable, spontaneous and genetically-induced mouse tumor models and
51 PD-L1 expression in cancer cells resulted in reduced NK cell responses and generation of more
52 aggressive tumors in vivo. PD-1 expression was more abundant on NK cells with an activated and
53 more responsive phenotype and did not mark NK cells with an exhausted phenotype. These
54 results demonstrate the importance of the PD-1/PD-L1 axis in inhibiting NK cell responses in vivo
55 and reveal that NK cells, in addition to T cells, mediate the effect of PD-1/PD-L1 blockade
56 immunotherapy.

57

58 **Main text**

59 **Introduction**

60 Immunotherapy targeting the PD-1/PD-L1 inhibitory axis has produced spectacular results in the
61 treatment of a wide variety of tumors (1-9). The current paradigm dictates that CD8 T cells are
62 inhibited by PD-1 and it is widely accepted that checkpoint blockade unleashes T cells to attack
63 tumor cells. However, many cancer types exhibit a high incidence of MHC loss and/or low
64 neoantigen burden (10, 11), which should render tumor cells refractory to recognition by CD8 T

65 cells. High levels of PD-L1 expression have been observed in tumors with low MHC I expression
66 (12-18). Interestingly, some of these cancer types are responsive to PD-1/PD-L1 blockade. An
67 example is Hodgkin's Lymphoma (12, 13), in which genes encoding PD-L1 are amplified.
68 Interestingly, in Hodgkin's Lymphoma, PD-L1 upregulation was predictive of a poor outcome even
69 when the tumor cells were defective in MHC I expression (19). These findings suggested the
70 existence of immune responses that are independent of cytotoxic T cells, inhibited by PD-1 and
71 rescued by PD-1-blockade.

72 NK cells are innate lymphocytes with cytotoxic activity against cancer cells that also
73 orchestrate the immune response by releasing cytokines and chemokines (20). NK cells participate
74 in the immune response against solid and hematopoietic cancers owing to their capacity to
75 recognize molecular patterns characteristic of stressed cells (so-called *missing-self* and *induced-*
76 *self* recognition (21)). NK cells mediate strong anti-leukemia activity when included in some
77 allogeneic stem cell transplants (22-31) and their presence in solid tumors is a good prognostic
78 factor (31-37). Unlike recognition by T cells, recognition by NK cells does not require that cancer
79 cells express neoantigens or over-express self-antigens, and loss of MHC expression on tumor
80 cells increases rather than decreases their susceptibility to NK cell killing (38, 39). Evidence that
81 PD-1 can be expressed on human NK cells has recently emerged in several cancer indications,
82 including Hodgkin's Lymphoma (40-44), but mechanistic in vivo studies examining whether and
83 how PD-1 inhibits NK cell responses to tumors, and whether PD-1/PD-L1 blockade mobilizes NK
84 cell responses, are still lacking.

85 Here, we investigated if the therapeutic effect of PD-1 and PD-L1 blockade relies on the
86 anti-tumor activity of NK cells. Using several cancer mouse models, we found that activated NK
87 cells express PD-1 and that PD-1 engagement by PD-L1⁺ tumor cells potently suppresses NK cell-
88 mediated immunity to tumors. Releasing PD-1-imposed inhibition through blockade of PD-1 or PD-
89 L1 activated an NK response that was indispensable for the full effect of PD-1/PD-L1 blockade.

90

91 **Results**

92 *NK cells participate in the therapeutic effect of PD-1/PD-L1 blockade:*

93 To study the effect of PD-1 blockade in a model where T cells do not participate in the
94 immune response against cancer, we took advantage of a lymphoma model based on injection of
95 RMA-S cells, which exhibit low expression of MHC I. Tumor surveillance of RMA-S cells is strongly
96 dependent on NK cells but not T cells (45), as confirmed by experiments where depletion of NK
97 cells, but not T cells, resulted in accelerated tumor growth (Figure 1A). RMA-S cells expresses low
98 levels of the PD-1 ligands PD-L1 and PD-L2, even after IFN- γ treatment in vitro (Figure 1B). Even
99 as established tumors in syngeneic mice, as tested in ex vivo tumor dissociates, expression of PD-
100 L1 by RMA-S cells was much lower than observed on myeloid cells in the spleen or on other tumor
101 cells such as the prostate adenocarcinoma line TRAMP-C2 (Figure 1C). We transduced RMA-S
102 cells with *Pdl1* and selected by flow cytometry cells with surface PD-L1 at levels comparable to
103 those observed on myeloid cells in the spleen or infiltrating the tumor, or to those naturally
104 expressed by a PD-L1⁺ tumor cell line in vivo (TRAMP-C2 cells, Figure 1B-C). Immunosurveillance
105 of RMA-S-*Pdl1* tumors was not mediated by T cells, but NK-depletion accelerated the growth of
106 tumor cells in vivo, showing that NK cells, but not T cells, mediate an immune response to this cell
107 line even when PD-L1 is expressed (Figure 1D). Therefore, this represents a valuable model to
108 study the effect of PD-1 blockade in a system where a CD8 T cell response to cancer cells is
109 incapacitated by low MHC expression, but an NK cell response is still evident.

110 To investigate whether PD-1/PD-L1 blockade elicits an effective response for tumors that
111 are insensitive to CD8 T cells, we injected RMA-S-*Pdl1* cells into B6 mice and after two days
112 treated the mice with a PD-1 blocking antibody (clone RMP1-14) (46). Mice treated just once
113 exhibited a markedly diminished rate of tumor progression (Figure 1E). However, when mice were
114 depleted of NK cells before tumor injection, the antibody treatment was completely ineffective

115 (Figure 1E), showing that PD-1 blockade mobilized an NK cell response. Next, we allowed the
116 RMA-S-*Pdl1* tumors to progress to a volume of ~25 mm³ before initiating treatment. Even in this
117 scenario, anti-PD-1 therapy significantly delayed tumor development (Figure 1F).

118 Compared to systemic injections, local injections of anti-PD-1 allow the use of a lower
119 antibody dose while potentially reducing systemic side effects. To address the efficacy of
120 intratumoral injection of therapeutic antibodies, RMA-S-*Pdl1* cells were mixed in Matrigel with
121 control Ig, PD-1 antibody (a dose more than 10-fold lower than in the systemic injection) or PD-L1
122 antibodies, and injected subcutaneously in B6 mice. Mice that received PD-1 or PD-L1 antibody in
123 the tumor inoculum developed significantly smaller tumors (Figure 1G-H), consistent with the
124 results obtained by injecting the antibody i.p.. Collectively, these data show that the efficacy of PD-
125 1 and PD-L1 blockade in MHC-deficient tumors depends on NK cell activity.

126

127 *PD-1 is expressed by and inhibits NK cells:*

128 Having shown that the efficacy of PD-1 and PD-L1 blockade depends on NK cells in a
129 scenario where tumor cells are MHC-deficient, we determined whether PD-1 was expressed by
130 and inhibited NK cells. We injected RMA-S cells in syngeneic mice and analyzed PD-1 expression
131 by flow cytometry. PD-1 was strongly upregulated on 30-40% of NK cells infiltrating RMA-S
132 tumors, but not in splenic NK cells (Figure 2A-B). PD-1 expression on intratumoral NK cells was
133 evident at the earliest time point that allowed dissection and analysis of the cells (day 7, when
134 tumors were small, <25 mm³). NK cells in the local lymph nodes draining the tumor, and in some
135 cases distant lymph nodes, showed slight PD-1 expression at early time points and higher
136 expression later (Figure 2A and not shown). Similar results were obtained when we analyzed NK
137 cells infiltrating tumors derived from the RMA tumor line, which is an MHC I⁺ version of RMA-S
138 cells (Figure 2C). Hence, PD-1 expression by NK cells within tumors is not limited to MHC-deficient
139 tumors.

140 Next, we employed another well-established tumor model based on s.c. injection of the
141 colon carcinoma cell line CT26 in syngeneic BALB/cJ mice. Up to 60% of NK cells infiltrating CT26
142 tumors expressed PD-1, whereas only modest PD-1 expression was observed on NK cells from
143 the draining lymph nodes, and no PD-1 expression was detected on splenic NK cells (Figure 2A-
144 C). PD-1 upregulation on NK cells was observed in numerous other tumor models including
145 several ectopic s.c. models and three spontaneous models (Figure 2C). Interestingly, we found
146 that PD-1 was expressed with a high degree of heterogeneity among tumor bearing mice both in
147 NK and CD8+ T cells (Figure 2C).

148 To study the functional effects of PD-1 engagement on NK cells, we initially used an in vitro
149 approach. Compared to untransduced tumor cells, tumor cells transduced with PD-L1 were less
150 effective in inducing degranulation and IFN- γ production by PD-1+ NK cells in vitro, consistent with
151 inhibition of NK activation by PD-L1 (Figure 2D-E). The prototypical NK-sensitive human target cell
152 line K562 lacks PD-L1 and PD-L2, and the human NK cell line NK92 lacks PD-1. Cytolysis of K562
153 cells by NK92 cells, and K562-induced degranulation of NK92 cells, were significantly reduced
154 when K562 and NK92 were transduced with PD-L1 and PD-1, respectively (Figure 1E, F).
155 Responses were minimally or not affected with empty vector-transduced NK92 cells, or when
156 NK92-*Pdcd1* (*Pdcd1* encodes PD-1) cells were stimulated with untransduced K562 cells,
157 demonstrating that inhibition required both receptor expression by NK cells and ligand expression
158 by target cells.

159 In conclusion, PD-1 is specifically upregulated by a population of NK cells in the tumor
160 microenvironment, and it suppresses NK cell degranulation and cytotoxic functions in vitro.

161

162 *PD-1 inhibits both NK- and T cell-mediated anti-tumor immunity:*

163 We investigated if PD-1 suppresses NK anti-tumor activity in vivo. In mice implanted with
164 10⁶ tumor cells, RMA-S-*Pd11* were much more aggressive than RMA-S cells (untransduced or

165 transduced with an empty vector) (Figure 3A). RMA-S-*Pd11* caused fatality in ~90% of recipients,
166 whereas only ~45% of mice injected with RMA-S cells developed fatal tumors (Figure 3B). NK-
167 depletion before tumor cell implantation (Figure 3B, C), or genetic depletion of NK cells in *Rag1*^{-/-}
168 *Il2rg*^{-/-} immuno-deficient mice (Figure 3D), resulted in similar growth of RMA-S and RMA-S-*Pd11*
169 tumors and similar rapid mortality, whereas depletion of CD4 and CD8 T cells had no effect (Figure
170 1A, D). These data verify the expectation that NK cells but not T cells mediate spontaneous
171 rejection of RMA-S cells, and indicate that in this model NK cells are inhibited by PD-1/PD-L1
172 interactions and rescued by PD-1/PD-L1 blockade. The finding that NK-depletion accelerated
173 tumor growth somewhat more potently than PD-L1 transduction of the RMA-S cells (Figure 3B, C)
174 suggests that while PD-L1 expression by RMA-S cells strongly inhibited NK cells, some residual
175 NK-mediated rejection still occurred.

176 RMA cells, unlike RMA-S, are resistant to NK cells, and also fail to provoke T cell-mediated
177 responses when inoculated in naïve mice (45, 47). Not surprisingly, RMA tumors grew rapidly in
178 B6 mice whether or not the tumor cells expressed PD-L1 (Figure 3E), demonstrating that PD-L1
179 protein expression by the tumor cells does not promote in vivo growth of tumors that are refractory
180 to NK- (and T cell-) mediated control.

181 Like RMA-S, the melanoma cell line B16-BL6 (hereafter abbreviated B16) is poorly
182 immunogenic for T cells but is sensitive to NK cells (48). We generated PD-L1-transductants of
183 B16 (hereafter abbreviated B16-*Pd11*). NK cells infiltrating subcutaneous B16 tumors expressed
184 PD-1 in only half of tumor-bearing animals, and at a low frequency (Figure 2C), so it was not
185 surprising that B16-*Pd11* cells grew at a similar rate in vivo as the parental cells when transferred
186 subcutaneously. In contrast, NK cells infiltrating lung tissue where B16 cells had colonized after i.v.
187 injection had appreciable, albeit variable, PD-1 expression (Figure 4B). Compared to the parental
188 cell line, B16-*Pd11* cells injected i.v. caused a more rapid disease, indicating that PD-L1 expression
189 inhibited tumor rejection (Figure 4C, E). Similar results were obtained with inocula of 5,000 or

190 20,000 tumor cells. With both doses, NK cell depletion accelerated the onset of lethal disease with
191 untransduced tumor cells to match the pace of disease with PD-L1-transduced tumor cells (Figure
192 4C-F). In contrast, CD8 depletion did not accelerate mortality in mice injected with B16 or B16-*Pdl1*
193 tumor cells (Sup. Figure 1). These data confirmed that B16 cells are controlled by NK cells and not
194 CD8 T cells (i.e. in the absence of immunotherapy), and indicated that higher PD-L1 expressed by
195 these tumor cells inhibits the NK cell response. Post-mortem analysis confirmed the higher degree
196 of tumor burden conferred by PD-L1 expression. Twenty-one days after injecting the lower dose of
197 tumor cells, only half of the mice that received B16 cells had macroscopically visible tumor
198 colonies in the lungs, whereas 12 out of 13 mice injected with B16-*Pdl1* cells had easily observable
199 lung tumors (Figure 4G). qRT-PCR analysis of lung tissue RNA for transcripts encoding a
200 melanocyte-specific protein (*Gp100(49)*) confirmed the increased burden of B16-*Pdl1* tumors as
201 compared to B16 cells (Figure 4H). We also attempted to address whether PD-1 blockade
202 provided a therapeutic effect in the B16 experimental metastasis model, but were stymied in the
203 effort by the failure of the PD-1 blocking antibody to efficiently penetrate the lung tumor
204 microenvironment, as indicated by the absence of antibody bound to PD-1⁺ cells in dissociated
205 tumors after treatment. Collectively, these findings indicated that PD-L1 expression inhibits NK-
206 mediated control of B16 lung colonization.

207 We investigated whether PD-1-mediated inhibition of NK cell responses was physiologically
208 relevant when T cells participated in anti-tumor immunity. Initially, we employed a tumor model
209 based on s.c. injection of CT26 cells in BALB/cJ mice. CT26 cells express high levels of ligands for
210 NK cell-activating receptors (Supplementary Figure 2) and are efficiently killed by IL-2-activated
211 NK cells in vitro (not shown). CT26 cells naturally express low amounts of PD-L1 in vitro, which is
212 strongly upregulated by IFN- γ (Figure 5A). To address the role of PD-1 inhibition in this tumor
213 model, we generated a PD-L1-deficient variant of CT26 by targeting the *Pdl1* gene with
214 CRISPR/Cas9. The mutation abolished PD-L1 expression whether or not the cells were treated

215 with IFN- γ (Figure 5A). When injected in BALB/cJ mice, CT26 cells generated solid tumors in all
216 recipients 5-7 days after injection, whereas growth of PD-L1-KO CT26 cells was dramatically
217 delayed, indicating that naturally expressed PD-L1 strongly inhibited the anti-tumor response
218 (Figure 5B). In this cancer model, PD-1 was upregulated on a large fraction of both NK and T cells
219 infiltrating the tumors (Figure 2C). To determine which immune cells were susceptible to PD-1-
220 mediated inhibition, groups of mice were depleted of NK cells, CD8 T cells, or both, before being
221 challenged with tumor cells. Notably, NK- or CD8-depletion resulted in substantial and similar
222 increases in the growth rates of CT26-*Pdl1*^{-/-} tumors, showing that PD-1 comparably inhibited NK
223 and CD8 T cells (Figure 5B). Furthermore, depletion of both NK and CD8 T cells resulted in even
224 faster tumor growth, comparable to the growth of wildtype CT26 cells, showing that NK cells and
225 CD8 T cells were the major tumor-rejecting populations, that they acted at least partly
226 independently, and that they were both inhibited by PD-L1 (Figure 5B). In contrast, with CT26
227 cells, depletion of NK and/or CD8 T cells had only a marginal effect on tumor growth (Figure 5C),
228 providing additional evidence that PD-L1 expressed by CT26 strongly inhibits both NK- and CD8-
229 mediated anti-tumor immunity.

230 As a control to show that the rejection of CT26-*Pdl1*^{-/-} cells was not due to off-target effects
231 incurred in preparing the mutants, or to the impact of the vector in the cells, we generated CT26-
232 *Pdl1*^{-/-} cells restored with PD-L1. PD-L1-transduced CT26-*Pdl1*^{-/-} cells expressed PD-L1 similarly
233 to WT cells treated with IFN- γ (Figure 5A), and grew as aggressively in vivo as wildtype CT26 cells,
234 whereas empty vector-transduced CT26-*Pdl1*^{-/-} cells were strongly rejected (Figure 5D). Together,
235 these data provide compelling evidence that the rejection of CT26-*Pdl1*^{-/-} cells was due to the PD-
236 L1 deficiency and not to other alterations in the cells.

237 As PD-1 restoration inhibited NK cells in the CT26-*Pdl1*^{-/-} model, we hypothesized that in
238 mice with CT26 tumors that express PD-L1, PD-1 blockade would reinvigorate an NK response

239 that would result in better tumor rejection. The increased tumor growth resulting from restoration of
240 PD-L1 expression in CT26-*Pdl1*^{-/-} cells (Figure 5D) was reversed when the animals were injected
241 with PD-L1 antibody (Figure 6A), indicating a therapeutic effect of PD-L1 blockade. The
242 therapeutic impact of PD-L1 blockade was impeded when NK cells were depleted in tumor-bearing
243 mice with two different treatment regimens (Figure 6B-C), showing that NK cells, in addition to CD8
244 T cells, contribute to the therapeutic effect of PD-L1 blockade.

245 To further corroborate these results, we employed a competitive in vivo killing assay. We
246 injected a 1:1 mixture of PD-L1-overexpressing and PD-L1-deficient CT26 cells in mice that were
247 depleted or not of NK cells. As shown in Figure 6D, the growth advantage of PD-L1-expressing
248 tumor cells observed in undepleted mice was lost when mice were depleted of NK cells, indicating
249 that NK cells preferentially kill tumor cells lacking PD-L1 expression.

250 Consistently, when CT26 tumors expressed PD-L1 the percentages of PD-1+ NK cells that
251 expressed the effector molecule granzyme B intracellularly were reduced as compared to PD-1+
252 NK cells in PD-L1-deficient CT26 tumors, or to PD-1- NK cells (Figure 6E). These data are
253 consistent with inhibition of NK effector function by PD-1-PD-L1 interactions in vivo. Moreover, PD-
254 L1 antibody treatment of mice bearing CT26 tumor cells resulted in a significant increase in the
255 percentage of granzyme B+ NK cells among PD-1+ NK cells, consistent with the impact of PD-L1
256 blockade on tumor rejection in vivo (Figure 6E). Several other parameters of NK cell activation
257 were unchanged, consistent with our observation that most NK activation markers are not strongly
258 induced by exposure to NK sensitive (as opposed to NK-resistant) tumors in vivo (MA and DHR,
259 unpublished observations). As CT26 cells are known to express high levels of MHC I molecules
260 and to express mutated neo-antigens (50), it was not surprising to observe such a strong T cell
261 response with the PD-L1-deficient variants. It is, however, remarkable that in such a scenario NK
262 cells play a comparable role to T cells and that with wildtype CT26 cells, PD-1 can potentially
263 suppress both responses.

264 As a fourth model, we employed orthotopic injections of 4T1 cells in the mammary fat pad
265 of BALB/cJ mice. Similarly to CT26 cells, 4T1 cells express NK cell-activating ligands and are
266 efficiently killed by IL-2-activated NK cells in vitro (Supplementary Figure 2 and data not shown).
267 We generated a PD-L1-deficient version of 4T1 cells (4T1-*Pdl1*^{-/-}) with CRISPR/Cas9 (Figure 7A).
268 When injected in BALB/cJ mice, 4T1 cells grew more rapidly than their PD-L1-deficient
269 counterpart, indicating that even in this model PD-L1 expression on tumor cells suppressed the
270 immune response (Figure 7B and D). As we observed with CT26-derived tumors, depletion of NK
271 or CD8 T cells separately did not completely rescue the growth of PD-L1-deficient tumor cells, but
272 concurrent depletion of NK and CD8 T cells accelerated the growth of 4T1-*Pdl1*^{-/-} cells to the level
273 observed with 4T1 cells, indicating that PD-L1 inhibition was exerted on both NK and CD8 T cells
274 (Figure 4B-E). Therefore, in two cancer models where CD8 T cells played a significant role, NK
275 responses were still important for controlling cancer development and PD-1 was able to suppress
276 the anti-tumor activity of NK cells.

277 These results in four different tumor models show that NK-mediated anti-tumor responses
278 are inhibited by PD-1, indicating that PD-1 represents an important checkpoint for NK cells.

279
280 *PD-1 is more abundantly expressed in activated NK cells with higher functional activity:*
281 NK cells are both phenotypically and functionally heterogeneous (20). In the analyzed tumor
282 models, PD-1 was expressed by a discrete fraction cells rather than by the entire population. We
283 addressed whether the NK cells that upregulated PD-1 correspond to a phenotypically defined
284 subset. Of the four maturation stages defined by CD27 and CD11b expression (51), PD-1 was
285 expressed on NK cells within all 4 stages, with somewhat higher expression on R2 cells
286 (CD11b⁺CD27⁺ NK cells), one of the stages of maturation where NK cells are more responsive
287 (Figure 8A).

288 Another element of heterogeneity among NK cells is provided by stochastic expression of
289 MHC-specific inhibitory receptors (20). In B6 mice, Ly49C, Ly49I and NKG2A recognize self MHC
290 I, whereas Ly49A and Ly49G2 do not (38). NK cells that expressed inhibitory receptors specific for
291 the host's MHC I molecules were marginally but significantly more likely to express PD-1. This was
292 evident when examining NK cells that simultaneously expressed all three of the known self MHC-
293 specific receptors (Ly49C⁺, Ly49I⁺, and NKG2A⁺) in B6 mice, or the larger population that
294 expressed at least one of the three (Figure 8B). Interestingly, NK cells expressing self MHC-
295 specific receptors exhibit greater functional responsiveness than other NK cells (38).

296 The more robust expression of PD-1 in NK cells with a phenotype associated with higher
297 responsiveness led us to hypothesize that cellular activation could be related to PD-1 expression.
298 Consistent with our hypothesis, NK cells that express activation markers like Sca-1 and CD69
299 consistently contained more PD-1⁺ NK cells than NK cells lacking these markers (Figure 8C-E).
300 Induction of PD-1 on NK cells did not, however, necessarily correlate with how well the tumor cells
301 stimulate NK cells. Indeed, PD-1 expression was similar on NK cells infiltrating RMA-S tumors (a
302 good NK cell target) and RMA tumors (an NK-resistant, MHC I-high sister cell line) (Figure 2C).
303 Moreover, compared to NK-insensitive RMA tumor cells, RMA cells that were rendered NK-
304 sensitive by transduction of the NK-activating ligands m157 or RAE-1 ϵ (which bind the Ly49H and
305 NKG2D activating receptors, respectively) induced only marginal increases in the percentage of
306 PD-1 expressing NK cells (Supplementary Figure 3). The lack of a strong association between
307 tumor cell stimulation of NK cells and PD-1 expression suggests that PD-1 upregulation may be
308 induced more potently by other types of signals, such as local exposure to generic activating or co-
309 activating ligands or cytokines.

310 The clear correlation between cellular activation markers and PD-1 expression prompted us
311 to investigate whether PD-1⁺ NK cells corresponded to the more functionally active NK cells. To
312 answer this question, we took advantage of an ex vivo approach, often used to assay NK cell

313 responsiveness (47, 52-54). We injected RMA-S or RMA-S-*Pd11* tumor cells in syngeneic B6 mice
314 and, after tumor formation re-stimulated tumor-infiltrating NK cells *ex vivo* with plate-bound
315 antibodies that crosslink NK cell activating receptors NKp46 or NKR-P1C, or isotype control
316 antibodies. Degranulation (CD107a on the cell surface) and intracellular accumulation of IFN- γ
317 were assessed. Interestingly, PD-1⁺ NK cells had substantially higher functional activity than PD-1-
318 negative NK cells (Figure 9). A similar result was obtained employing NK cells infiltrating PD-L1+
319 or PD-L1- CT26 tumors (Figure 10). These results showed that PD-1 is selectively upregulated on
320 the most activated and functionally responsive intratumoral NK cells. These findings explain why
321 the NK response is potently suppressed by PD-1 interactions when PD-1 is only expressed by a
322 fraction of NK cells: the PD-1+ NK cells are the ones with the greatest potential activity and are
323 responsible for most of the response when PD-1 interactions are blocked.

324 In conclusion, our studies show that PD-1/PD-L1 blockade relies on NK cells in both MHC+
325 and MHC- tumors. PD-1 inhibits NK-dependent immune surveillance and favors the escape of
326 tumor cells from NK cell responses.

327

328 **Discussion:**

329 The efficacy of PD-1 blockade has been correlated with reinvigoration of a pre-existing T cell
330 response (55). Indeed, tumors with abundant neoantigens due to an elevated mutational load,
331 such as melanomas and lung cancers, tend to be more responsive to PD-1 blockade than tumors
332 with a low somatic mutation load (56-59). However, the prevalent view that T cells are the only
333 important mediators of the anti-tumor response unleashed by PD-1 blockade is challenged by at
334 least two observations: *i*) human tumors often lose expression of HLA-I molecules (10, 60), and in
335 some of these tumors PD-1 blockade is still effective; *ii*) a strong clinical response to PD-1
336 blockade is observed in tumor indications, such as Hodgkin's lymphomas, that display extremely
337 low mutational loads (12, 13). Unlike T cells, NK cells can respond to MHC-deficient tumors (45)

338 and they are activated by ligands that are usually upregulated upon oncogenic stress (39, 61).
339 Based on these premises, we hypothesized that PD-1 blockade may activate an NK cell response.

340 Tumors that are good T cell targets, such as melanoma and lung cancer cells, also express
341 high levels of ligands for NK-activating receptors (62-65). Furthermore, NK cells often infiltrate
342 melanoma and lung tumors. Hence, NK cells may also participate in immune-mediated rejection of
343 these tumors, even if T cells may play a major role under these conditions.

344 Here, we present the first mechanistic evidence that PD-1 blockade elicits an anti-tumor NK
345 cell response and that PD-1 is an important checkpoint for NK activation. We propose that along
346 with T cells, NK cells also participate in the clinical benefit of PD-1/PD-L1 antibody therapy. NK
347 cells may participate by helping to recruit a T cell response and/or by killing tumor cells directly.
348 The participation of T cells vs NK cells in direct tumor killing will likely depend on the relative
349 sensitivity of the specific tumor to NK versus T cells, which in turn varies depending on numerous
350 factors including expression of MHC I and activating ligands for NK cells, the antigenic load of the
351 tumor cells, PD-L1 expression by the tumor cells, and PD-1 expression by NK cells and T cells in
352 the tumor bed. Our studies in mice, for example, show that PD-1 blockade elicits anti-tumor
353 responses by both T cells and NK cells in the case of CT26 tumors, whereas it elicits an NK cell
354 response in the case of RMA-S-*Pdl1* tumors, which are defective for MHC I expression.
355 Interestingly, ~79% of classical Hodgkin's lymphomas show decreased or absent expression of
356 MHC I (19), yet a large majority of patients respond to PD-1 blockade immunotherapy (12). These
357 observations suggest the possibility that NK cells participate in tumor elimination stimulated by PD-
358 1 immunotherapy in this indication and probably others. Other immune cell types such as tumor-
359 associated macrophages, may also express PD-1 and may also play a role in therapeutic
360 responses (66). Interestingly, PD-1 expression has been detected on human NK cells in several
361 cancer indications (40-43). Though NK cells exhibit cytotoxicity against many tumors, they fail to
362 eliminate many tumors in vivo, and are frequently found in tumor beds in an inactive state. Based

363 on the collective data, we believe that PD-1 engagement is at least partially responsible for the
364 impact of PD-L1 expression by tumor cells on NK-dependent tumor rejection. However, PD-1
365 expressed by cells other than NK cells and CD8 T cells may also play a role, depending on the
366 tumor type and the nature of the immune response. The same reasoning likely applies to other
367 checkpoint receptors, including LAG-3, TIM-3 and TIGIT, that probably play a wider role in the
368 tumor microenvironment than inhibiting T cells.

369 Functional and phenotypic tests showed that the PD-1⁺ NK cells had the highest functional
370 activity when stimulated *ex vivo* and were largely included in the subsets of NK cells that
371 expressed activation markers (CD69 and Sca-1). These data suggest that PD-1⁺ NK cells are not
372 necessarily anergic in PD-L1⁺ tumors but may instead be inhibited in killing tumor cells. Studies
373 suggest that anergy and PD-1 expression are independent processes in T cells as well (67) and it
374 was recently reported that activation, rather than exhaustion, drives expression of PD-1 and other
375 checkpoint receptors on human T cells (68). PD-1-negative NK cells may fail to kill tumor cells
376 because they failed to become activated or have been rendered anergic. Whatever the
377 explanation, the finding that PD-1⁺ NK cells are the most active provides a plausible explanation
378 for why PD-L1 expression by tumor cells suppresses the response even though only a fraction of
379 NK cells expressed PD-1. Furthermore, it is consistent with the impact of PD-1 and PD-L1
380 blockade, because these more active NK cells would be expected to vigorously attack tumor cells
381 once the inhibitory interaction is disrupted.

382 PD-1 expression by CD8 T cells is also correlated with activation (68). Unexpectedly, PD-1
383 expression by NK cells occurred even within tumors that are poor targets for NK cells *in vitro*, such
384 as from the RMA tumor line. PD-1 expression trended higher, but not appreciably so, within tumors
385 formed from RMA transfectants that expressed NK activating ligands. The data suggest that PD-1
386 expression is induced by other activating signals or a combination of them, supplied within tumors.
387 Cytokine cocktails we have tested were not sufficient to induce PD-1 on NK cells (data not shown).

388 It will be important in future studies to identify the mechanisms that lead to PD-1 expression by NK
389 cells in tumors, and the source of variation in PD-1 expression in different tumors.

390 Our results, and those of others (69, 70), suggest there are opportunities for combining PD-1 or
391 PD-L1 antibody therapy with agents that enhance the anti-tumor effects of NK cells by other
392 means including KIR blockade (71), cytokine therapy (47), ADCC (72) and other mechanisms (73)
393 for marshaling NK cell responses against cancer. Finally, given reports that NK cells express other
394 checkpoint receptors, such as CTLA-4, LAG-3, CD96 and TIGIT (74-76), therapies targeting those
395 molecules may also mobilize NK responses and will be subject of future studies.

396

397 **Materials and Methods:**

398 **Mice and in vivo procedures**

399 Mice were maintained at the University of California, Berkeley or at the University of
400 Ottawa, ON. C57BL/6J, BALB/cJ, and *Rag1^{-/-}Il2rg^{-/-}* were bred from mice purchased from The
401 Jackson Laboratory and B6-*Klrk1^{-/-}* mice were described (77). *p53^{fl/fl}* mice and *Kras^{+LSL-G12D}* mice,
402 both purchased from Jackson Laboratory, were bred to generate KP (*Kras^{+LSL-G12D}p53^{fl/fl}*) mice
403 (78). *Ncr1^{+gfp}* mice were a gift of Dr. Mandelboim (Hebrew University, Jerusalem, Israel). For all
404 experiments, sex- (both males and females) and age- (six- to twelve-week old) matched mice were
405 employed.

406 For s.c. and orthotopic injections, tumor cells resuspended in 100 μ l of RPMI without FCS
407 were injected in the left flank or in the mammary fat pad. Tumor growth was monitored by caliper
408 measurements. For the experimental metastasis model, tumor cells resuspended in 200 μ l of
409 RPMI without FCS were injected intra-venously in the tail vein. KP sarcomas were induced by
410 intramuscular hind leg injection of 25,000 PFU of a lentivirus expressing Cre recombinase in a
411 volume of 50 μ l. Cre-expressing lentivirus was produced in 293T cells by simultaneous transfection

412 of a transfer vector encoding Cre (a gift from Tyler Jacks, MIT, Boston, MA) along with the
413 plasmids psPAX2 and pCMV-VSV-G. Cell culture supernatant containing Lenti-Cre was passed
414 through a 0.45 μ M filter, centrifuged at 20,000 RPM, and resuspended in a 1:1 mixture of HBSS
415 and OptiMem. Viral preparations were titered using the GreenGO reporter cell line (Tyler Jacks,
416 MIT, Boston, MA).

417 To deplete CD8 T cells, mice were injected i.p. with 250 μ g of monoclonal antibodies H35-
418 17.2 (specific for CD8 β) or 2.43 (specific for CD8 α) on day -2 and -1 relative to tumor injection.
419 CD4 T cells were depleted by i.p. injection of 500 μ g of GK1.5 monoclonal antibodies (specific for
420 CD4) on days -3 and -1. To deplete NK cells in C57BL/6 mice, 250 μ g of PK136 (specific for NKR-
421 P1C) were injected i.p. on day -1 and -2. In BALB/cJ mice, 10 μ l of anti-asialoGM1 were injected
422 i.p. on days -2 and -1. Cell depletion was confirmed by staining peripheral blood cells with
423 antibodies different than the ones used for in vivo depletion. Specifically, NK-depletion was
424 confirmed by the absence of CD3⁺NKp46⁺ cells, CD8 T cell depletion was confirmed by the
425 absence of CD3⁺CD4⁻ cells and CD4 T cell depletion was confirmed by the absence of CD3⁺CD8⁻
426 cells.

427 For experiments using RMA-S or RMA-S-*Pd11* cells, checkpoint blockade was performed
428 by injecting 250 μ g of PD-1 (RMP1-14) or PD-L1 (10F.9G2) antibodies, or control IgG, i.p. In one
429 protocol, the antibody was delivered two days after tumor cell injection. In a second protocol, the
430 antibody was injected when the tumor volume reached 25 mm³, and repeated two days after. In a
431 third protocol, tumor cells were injected s.c. after resuspending the cells in 100 μ l of Growth Factor
432 Reduced MATRIGEL (BD) mixed with 20 μ g of control or PD-1 or PD-L1 antibodies.

433 For experiments using CT26-*Pd11*^{-/-} cells transduced with empty vector or *Pd11* expression
434 vector, checkpoint blockade was performed by injecting 250 μ g of PD-L1 (10F.9G2) antibodies, or
435 control IgG i.p., daily from day 1 to day 10 after injecting tumor cells. In these mice, immune

436 depletion was performed at day -2, -1, 7 and 14. In a second protocol, PD-L1 antibody was
437 injected at day 3, 4, 5, 7 and 10. In these animals, NK depletion was performed at day 2, 9 and 16.

438

439 **Cell lines and cell culture**

440 All cell lines were cultured at 37°C in humidified atmosphere containing 5% CO₂ with media
441 containing 100 U/mL penicillin, 100 µg/mL streptomycin, 0.2 mg/mL glutamine, 10 µg/mL
442 gentamycin sulfate, 20 mM HEPES and 5% FCS (10% FCS in the case of CT26 cells). RMA, RMA-
443 *Pdl1*, RMA-S, RMA-S-*Pdl1*, RMA-*m157*, RMA-RAE-1ε, C1498, CT26, CT26-*Pdl1*^{-/-}, K562, K562-
444 *Pdl1*, A20, YAC-1, YAC-1-*Pdl1*, 4T1 and 4T1-*Pdl1*^{-/-} were cultured in RPMI whereas B16, B16-*Pdl1*
445 and TRAMP-C2 were cultured in DMEM. NK92 and NK92-*Pdcd1* were cultured in MEM-α with
446 10% FCS, 10% Horse Serum, 100 U/ml recombinant human IL-2, 100 U/mL penicillin, 100 µg/mL
447 streptomycin, 0.2 mg/mL glutamine, 10 µg/mL gentamycin sulfate, and 20 mM HEPES. Cell line
448 identify was confirmed by flow cytometry or PCR and tested negative for mycoplasma.

449

450 **Flow cytometry**

451 In mice injected with tumor cells s.c., or in the sarcoma model, draining lymph nodes
452 (inguinal), non-draining lymph nodes (brachial LN) and spleens were gently dissociated through a
453 40 µm filter and the resulting single cell suspensions were employed for experiments. The tumors
454 were excised after separating the skin, cut in pieces and dissociated using a gentleMACS
455 Dissociator (Miltenyi). In mice injected with tumor cells i.v., lungs were perfused and then
456 dissociated using a gentleMACS Dissociator. Cell preparations from tumors and lungs were loaded
457 on a mouse-lympholyte gradient (Cedarlane) and then stained. TRAMP and Eu-Myc derived
458 tumors were dissociated with collagenase and cells were stored frozen at -80° C. Before staining,
459 cells were thawed and loaded on a mouse-lympholyte gradient.

460 Dead cells were excluded by staining with Live-Dead fixable stain kit (Molecular Probes) for
461 30 min. Cells were then incubated for 20 min with 2.4G2 hybridoma supernatant to block FcγRII/III
462 receptors and for a further 20 min primary specific antibodies, before washing. When necessary,
463 an additional incubation with fluorochrome-conjugated streptavidin (Biolegend) was performed and
464 the samples were subjected to flow cytometric analysis. For intracellular staining of IFN-γ and
465 granzyme B, we used the Cytotfix/Cytoperm kit (BD), following the manufacturer's instructions.

466 Multicolor flow cytometry was performed with an LSRFortessa (BD) or with an X20-
467 Fortessa (BD), and data were analyzed with the FlowJo software (Tree Star Inc.).

468

469 **Antibodies**

470 For flow cytometry we used the following antibodies (clone names are in parentheses).
471 From Biolegend: anti-CD3ε (145-2C11), anti-CD4 (GK1.5), anti-CD11b (M1/70), CD11c (N418),
472 anti-CD19 (6D5), anti-CD69 (H1.2F3), anti-CD137 (4-1BB, clone 17B5), anti-DNAM (10E5), anti-
473 F4/80 (BM8), anti-Ly6C (HK1.4), anti-Ly6G (1A8), anti-Ly49A (YE1/48.10.6), anti-NKp46 (29A1.4),
474 anti-NKR-P1C (PK136), anti-PD-1 (29F.1A12), anti-PD-L1 (10F.9G2), anti-PVR (TX56), anti-Sca-1
475 (D7), anti-Ter119 (TER-119), rat-IgG2a isotype control. From eBioscience: anti-CD25 (PC61.5),
476 anti-CD27 (37.51), anti-CD45.1 (A20), anti-CD45.2 (104), anti-Ki67 (SolA15), anti-mouse CD107a
477 (eBio1D4B), anti-human CD107a (eBioH4A3), anti-KLRG1 (2F1), anti-Ly49G2 (LGL-1), anti-MHC
478 class I H-2D^b (28.14.8), anti-MHC class I H-2K^d (SF1-1.1.1), anti-NKG2A/C/E (20d5), anti-NKG2D
479 (MI-6). From BD Pharmingen: anti-CD25 (PC61), anti-Ly49I (YLI-90) and anti-granzyme B (GB11).
480 From R&D Systems: anti-H60 (205326), anti-MULT1 (237104), anti-Nectin2 (829038) anti-pan-
481 RAE-1 (186107). Anti-Ly49C (4LO3311) was a gift from S. Lemieux, l'Institut national de la
482 recherche scientifique—Institut Armand-Frappier (Laval, QC). Anti-m157 (6H121) was a gift from W.
483 Yokoyama, Washington University School of Medicine (St. Louis, MO).

484 Antibodies for in vivo depletions or in vivo treatments were obtained from Leinco (St. Louis,
485 MO) except for anti-asialoGM-1 obtained from Biolegend.

486

487 **Viral Transduction**

488 A cDNA clone encoding wild type mouse *Pdl1* (gene ID 60533) was subcloned into the
489 pQCXIN (provided by L. Coscoy, University of California, Berkeley) or MSCV-IRES-Thy1.1-DEST
490 (Addgene 17442) retroviral expression vectors. A cDNA clone encoding wild type mouse *Pdcd1*
491 (gene ID 18566) was subcloned into the 236pHAGE.EF1A expression vector, provided by R. Tjian
492 at the University of California, Berkeley, CA. Cells expressing the vector were selected based on
493 mCherry expression. *m157*-encoding plasmid was a gift of J. Sun, Memorial Sloan Kettering
494 Cancer Center (New York, NY). Expression plasmids were amplified in DH5 α bacterial cells and
495 purified by midi-prep (Quiagen).

496 Retro- and lenti-viral expression vectors were generated by transfecting 293T cells with 2
497 μ g of vector with 2 μ g of packaging+polymerase-encoding plasmids using Lipofectamine 2000.
498 Virus-containing supernatants were used to transduce target cells by spin-infection (800xg for 2
499 hours at 37°C) with 8 μ g/ml of Polybrene. Transduced cells were sorted using an Influx cell sorter
500 or selected by culturing them in medium containing 1 mg/ml of G418 for 48 hours, as indicated.

501

502 **Generation of PD-L1-deficient mutants of the CT26 and 4T1 cell lines.**

503 Single guide (sg) RNA targeting the third exon of the *Pdl1* gene (sequence:
504 GTATGGCAGCAACGTCACGA) was cloned into the LentiCRISPR lentiviral backbone vector, also
505 containing the *Cas9* gene. CT26 or 4T1 cells were transfected with 2 μ g of plasmid and after 2
506 days were treated with 20 ng/ml of recombinant mouse IFN- γ (Peprotech). After 48 hrs, cells that
507 failed to upregulate PD-L1 were sorted. IFN- γ treatment and cell sorting were repeated for three

508 cycles, after growing the cells for 5 days after each treatment. Cells were cultured extensively in
509 the absence of IFN- γ before use.

510

511 **Flow cytometry based killing assay**

512 15,000 CFSE-labeled target cells were incubated for 5 hours with effector cells at different
513 E:T ratios in 96 well U bottom plates in technical triplicates. Cells were then stained with the
514 Live/Dead Fixable viability dye (Molecular probes) and resuspended in 150 μ l of flow buffer. 8,000
515 APC-labelled microbeads (Bangs Laboratories) resuspended in 50 μ l were added to each well. 180
516 μ l of cells+beads were acquired at the flow cytometer using the HTS plate reader. The ratio among
517 viable target cells (defined as CFSE⁺viability dye⁻ cells) and fluorescent microbeads (defined as
518 APC⁺ events) was calculated in each well (T/B). %Specific lysis was calculated for each well as:

519 %Specific lysis= $(T/B^{\text{experimental condition}} - T/B^{\text{target alone}})/(T/B^{\text{target+bleach}} - T/B^{\text{target alone}}) \times 100$

520

521 **Degranulation assay**

522 Splenocytes from resting *Ncr1^{+gfp}* mice (all NK cells express GFP) were spin infected twice
523 (at day 0 and day 1) with *Pdcd1*-encoding lentivirus in the presence of 1000 U/ml of recombinant
524 human IL-2. On day 2, activated splenocytes were harvested, stained with cell trace violet
525 (Biolegend) and used as effectors in a degranulation assay. 30,000 effector cells were cultured
526 with RMA-S or RMA-S-*Pd11* cells at different T:E ratios for 5 hrs with 1 μ g of Golgi Plug (BD), 1 μ g
527 of Golgi Stop (BD), and anti-CD107a. PD-1 staining was performed after the stimulation. NK cells
528 were gated as viable-cell trace violet⁺GFP⁺.

529 NK92-*Pdcd1* and NK92 cells transduced with empty vector were CFSE-labeled and used
530 as effectors in a degranulation assay. 20,000 effectors cells were stimulated with K562 or
531 K562/*Pd11* cells at different T:E ratios for 5 hrs with 1 μ g of Golgi Stop and anti-CD107a.

532 In other experiments, wells of flat-bottomed high-protein-binding plates were coated with
533 0.5 µg of control isotype or NKp46 antibody or 5 µg of NKR-P1C antibody. ~10⁶ tumor-infiltrating
534 cells were stimulated in the presence of 100 U of recombinant human IL-2, anti-CD107a, 1 µg of
535 Golgi Plug and 1 µg of Golgi Stop. After 5 hours, cells were harvested, stained with anti-PD-1, and
536 degranulation and IFN-γ accumulation on PD-1+ vs PD-1- NK cells was assessed by flow
537 cytometry.

538

539 **RNA isolation, reverse transcription, and quantitative PCR**

540 Lungs from control or from mice injected with B16 tumor variants were dissociated using a
541 gentleMACS Dissociator and RNA was extracted using the RNeasy Mini Kit (Qiagen). RNA
542 preparations were treated with DNase I (DNA-free Kit, Invitrogen) for 25 minutes at 37°C before
543 retro-transcribing 1 µg of RNA using the iScript reverse transcriptase system (Bio-Rad).
544 Quantitative real-time PCR was performed on a CFX96 thermocycler (Bio-Rad) using SSO-Fast
545 EvaGreen Supermix (Bio-Rad). *B-actin* mRNA and *Rlt19* rRNA were used as references.

546 Primers sequences:

547 *Gp100*:

548 FW: AGCACCTGGAACCCACATCTA

549 RV: CCAGAGGGCGTTTGTGTAGT

550 *B-actin*:

551 FW: AGAGGGAAATCGTGCGTGAC

552 RV: CAATAGTGACCTGGCCGT

553 *Rtl19*:

554 FW: GGCAGTACCCTTCCTCTTCC

555 RV: AGCCTGTGACTGTCCATTCC

556

557 **Statistics**

558 Statistical analysis was performed with the two-tailed unpaired (or paired when indicated)
559 Student's *t*-tests or Mann-Whitney tests or with one- or two-way ANOVA. Survival experiments
560 were analyzed with log-rank test. Values <0.05 were considered statistically significant. Different
561 experimental groups were equally allocated among the same cage (5-6 mice/small cage, up to 12
562 mice in large cage). No experimental blinding was necessary. In all experiments, when statistical
563 analyses were performed, the compared groups had similar variance.

564

565 **Study approval:**

566 All the experiments were reviewed and approved by the Animal Care and Use Committee
567 at the University of California, Berkeley, (Berkeley, CA) in accordance with the guidelines of the
568 National Institutes of Health and by the Animal Care Veterinary Services at the University of
569 Ottawa, (Ottawa, ON) in accordance with the guidelines of the Canadian Institutes of Health
570 Research.

571

572

573 **Author Contributions:**

574 MA, JH, JJH, MM, MCB and CJN performed and analyzed the experiments. TNT, CSA,
575 AKS, HER, TWT, LZ, AI, KEJ, NM, GAK, MWM and JCB assisted with the experiments. MA and
576 DHR conceived of the study, designed and interpreted the experiments and prepared the
577 manuscript. All authors critically read the manuscript.

578

579 **Acknowledgements**

580 We thank Hector Nolla, Alma Valeros and Vera Tang for help with cell sorting, Francesco
581 Spallotta and Dr. Cencioni for help with q-PCR analyses and members of the Raulet Lab and
582 Ardolino Lab for discussions. Dr. Giuseppe Sciumè critically read the manuscript. MA was
583 supported by an Istituto Pasteur-Fondazione Cenci Bolognetti post-doctoral fellowship, and by a
584 CRI Irvington Fellowship. JH and CSA were supported by summer undergraduate research
585 fellowships from Rose Hill. TWT was supported by a Student Training in Tumor Immunology
586 Fellowship from the Cancer Research Institute. This work was supported by NIH grants R01-
587 CA093678 and R01-AI113041 to DHR and by a Telus Ride for Dad grant from the Prostate Cancer
588 Fight Foundation and a CIHR project grant to MA.

589

590 **References:**

- 591 1. Topalian SL, Hodi FS, Brahmer JR, Gettinger SN, Smith DC, McDermott DF, et al. Safety,
592 activity, and immune correlates of anti-PD-1 antibody in cancer. *N Engl J Med.*
593 2012;366(26):2443-54.
- 594 2. Brahmer JR, Tykodi SS, Chow LQ, Hwu WJ, Topalian SL, Hwu P, et al. Safety and activity
595 of anti-PD-L1 antibody in patients with advanced cancer. *N Engl J Med.*
596 2012;366(26):2455-65.
- 597 3. Hamid O, Robert C, Daud A, Hodi FS, Hwu WJ, Kefford R, et al. Safety and tumor
598 responses with lambrolizumab (anti-PD-1) in melanoma. *N Engl J Med.* 2013;369(2):134-
599 44.
- 600 4. Callahan MK, Postow MA, and Wolchok JD. CTLA-4 and PD-1 Pathway Blockade:
601 Combinations in the Clinic. *Frontiers in oncology.* 2014;4:385.
- 602 5. Robert C, Ribas A, Wolchok JD, Hodi FS, Hamid O, Kefford R, et al. Anti-programmed-
603 death-receptor-1 treatment with pembrolizumab in ipilimumab-refractory advanced
604 melanoma: a randomised dose-comparison cohort of a phase 1 trial. *Lancet.*
605 2014;384(9948):1109-17.
- 606 6. Tumeh PC, Harview CL, Yearley JH, Shintaku IP, Taylor EJ, Robert L, et al. PD-1
607 blockade induces responses by inhibiting adaptive immune resistance. *Nature.*
608 2014;515(7528):568-71.
- 609 7. Herbst RS, Soria JC, Kowanetz M, Fine GD, Hamid O, Gordon MS, et al. Predictive
610 correlates of response to the anti-PD-L1 antibody MPDL3280A in cancer patients. *Nature.*
611 2014;515(7528):563-7.
- 612 8. Powles T, Eder JP, Fine GD, Braiteh FS, Loriot Y, Cruz C, et al. MPDL3280A (anti-PD-L1)
613 treatment leads to clinical activity in metastatic bladder cancer. *Nature.*
614 2014;515(7528):558-62.

- 615 9. Robert C, Long GV, Brady B, Dutriaux C, Maio M, Mortier L, et al. Nivolumab in
616 previously untreated melanoma without BRAF mutation. *N Engl J Med.* 2015;372(4):320-
617 30.
- 618 10. Garrido F, and Algarra I. MHC antigens and tumor escape from immune surveillance. *Adv*
619 *Cancer Res.* 2001;83:117-58.
- 620 11. Aptsiauri N, Cabrera T, Garcia-Lora A, Lopez-Nevot MA, Ruiz-Cabello F, and Garrido F.
621 MHC class I antigens and immune surveillance in transformed cells. *Int Rev Cytol.*
622 2007;256:139-89.
- 623 12. Ansell SM, Lesokhin AM, Borrello I, Halwani A, Scott EC, Gutierrez M, et al. PD-1
624 blockade with nivolumab in relapsed or refractory Hodgkin's lymphoma. *N Engl J Med.*
625 2015;372(4):311-9.
- 626 13. Ansell SM. Hodgkin lymphoma: MOPP chemotherapy to PD-1 blockade and beyond. *Am J*
627 *Hematol.* 2016;91(1):109-12.
- 628 14. Zaretsky JM, Garcia-Diaz A, Shin DS, Escuin-Ordinas H, Hugo W, Hu-Lieskovan S, et al.
629 Mutations Associated with Acquired Resistance to PD-1 Blockade in Melanoma. *N Engl J*
630 *Med.* 2016;375(9):819-29.
- 631 15. Smahel M. PD-1/PD-L1 Blockade Therapy for Tumors with Downregulated MHC Class I
632 Expression. *Int J Mol Sci.* 2017;18(6).
- 633 16. Aust S, Felix S, Auer K, Bachmayr-Heyda A, Kenner L, Dekan S, et al. Absence of PD-L1
634 on tumor cells is associated with reduced MHC I expression and PD-L1 expression
635 increases in recurrent serous ovarian cancer. *Sci Rep.* 2017;7:42929.
- 636 17. McGranahan N, Rosenthal R, Hiley CT, Rowan AJ, Watkins TBK, Wilson GA, et al.
637 Allele-Specific HLA Loss and Immune Escape in Lung Cancer Evolution. *Cell.*
638 2017;171(6):1259-71 e11.
- 639 18. Marty R, Kaabinejadian S, Rossell D, Slifker MJ, van de Haar J, Engin HB, et al. MHC-I
640 Genotype Restricts the Oncogenic Mutational Landscape. *Cell.* 2017;171(6):1272-83 e15.
- 641 19. Roemer MG, Advani RH, Redd RA, Pinkus GS, Natkunam Y, Ligon AH, et al. Classical
642 Hodgkin Lymphoma with Reduced beta2M/MHC Class I Expression Is Associated with
643 Inferior Outcome Independent of 9p24.1 Status. *Cancer Immunol Res.* 2016;4(11):910-6.
- 644 20. Vivier E, Raulet DH, Moretta A, Caligiuri MA, Zitvogel L, Lanier LL, et al. Innate or
645 adaptive immunity? The example of natural killer cells. *Science.* 2011;331(6013):44-9.
- 646 21. Marcus A, Gowen BG, Thompson TW, Iannello A, Ardolino M, Deng W, et al. Recognition
647 of tumors by the innate immune system and natural killer cells. *Adv Immunol.* 2014;122:91-
648 128.
- 649 22. Ruggeri L, Capanni M, Casucci M, Volpi I, Tosti A, Perruccio K, et al. Role of natural killer
650 cell alloreactivity in HLA-mismatched hematopoietic stem cell transplantation. *Blood.*
651 1999;94(1):333-9.
- 652 23. Giebel S, Locatelli F, Lamparelli T, Velardi A, Davies S, Frumento G, et al. Survival
653 advantage with KIR ligand incompatibility in hematopoietic stem cell transplantation from
654 unrelated donors. *Blood.* 2003;102(3):814-9.
- 655 24. Beelen DW, Ottinger HD, Ferencik S, Elmaagacli AH, Peceny R, Trenscher R, et al.
656 Genotypic inhibitory killer immunoglobulin-like receptor ligand incompatibility enhances
657 the long-term antileukemic effect of unmodified allogeneic hematopoietic stem cell
658 transplantation in patients with myeloid leukemias. *Blood.* 2005;105(6):2594-600.

- 659 25. Verheyden S, Schots R, Duquet W, and Demanet C. A defined donor activating natural
660 killer cell receptor genotype protects against leukemic relapse after related HLA-identical
661 hematopoietic stem cell transplantation. *Leukemia*. 2005;19(8):1446-51.
- 662 26. Miller JS, Cooley S, Parham P, Farag SS, Verneris MR, McQueen KL, et al. Missing KIR
663 ligands are associated with less relapse and increased graft-versus-host disease (GVHD)
664 following unrelated donor allogeneic HCT. *Blood*. 2007;109(11):5058-61.
- 665 27. Kim HJ, Choi Y, Min WS, Kim TG, Cho BS, Kim SY, et al. The activating killer cell
666 immunoglobulin-like receptors as important determinants of acute graft-versus host disease
667 in hematopoietic stem cell transplantation for acute myelogenous leukemia.
668 *Transplantation*. 2007;84(9):1082-91.
- 669 28. Willemze R, Rodrigues CA, Labopin M, Sanz G, Michel G, Socie G, et al. KIR-ligand
670 incompatibility in the graft-versus-host direction improves outcomes after umbilical cord
671 blood transplantation for acute leukemia. *Leukemia*. 2009;23(3):492-500.
- 672 29. Giebel S, Nowak I, Dziaczekowska J, Czerw T, Wojnar J, Krawczyk-Kulis M, et al.
673 Activating killer immunoglobulin-like receptor incompatibilities enhance graft-versus-host
674 disease and affect survival after allogeneic hematopoietic stem cell transplantation. *Eur J*
675 *Haematol*. 2009;83(4):343-56.
- 676 30. Cooley S, Weisdorf DJ, Guethlein LA, Klein JP, Wang T, Le CT, et al. Donor selection for
677 natural killer cell receptor genes leads to superior survival after unrelated transplantation for
678 acute myelogenous leukemia. *Blood*. 2010;116(14):2411-9.
- 679 31. Malmberg KJ, Carlsten M, Bjorklund A, Sohlberg E, Bryceson YT, and Ljunggren HG.
680 Natural killer cell-mediated immunosurveillance of human cancer. *Semin Immunol*. 2017.
- 681 32. Coca S, Perez-Piqueras J, Martinez D, Colmenarejo A, Saez MA, Vallejo C, et al. The
682 prognostic significance of intratumoral natural killer cells in patients with colorectal
683 carcinoma. *Cancer*. 1997;79(12):2320-8.
- 684 33. Ishigami S, Natsugoe S, Tokuda K, Nakajo A, Che X, Iwashige H, et al. Prognostic value of
685 intratumoral natural killer cells in gastric carcinoma. *Cancer*. 2000;88(3):577-83.
- 686 34. Villegas FR, Coca S, Villarrubia VG, Jimenez R, Chillon MJ, Jareno J, et al. Prognostic
687 significance of tumor infiltrating natural killer cells subset CD57 in patients with squamous
688 cell lung cancer. *Lung cancer*. 2002;35(1):23-8.
- 689 35. Schleypen JS, Baur N, Kammerer R, Nelson PJ, Rohrmann K, Grone EF, et al. Cytotoxic
690 markers and frequency predict functional capacity of natural killer cells infiltrating renal cell
691 carcinoma. *Clinical cancer research : an official journal of the American Association for*
692 *Cancer Research*. 2006;12(3 Pt 1):718-25.
- 693 36. McKay K, Moore PC, Smoller BR, and Hiatt KM. Association between natural killer cells
694 and regression in melanocytic lesions. *Hum Pathol*. 2011;42(12):1960-4.
- 695 37. Pasero C, Gravis G, Granjeaud S, Guerin M, Thomassin-Piana J, Rocchi P, et al. Highly
696 effective NK cells are associated with good prognosis in patients with metastatic prostate
697 cancer. *Oncotarget*. 2015;6(16):14360-73.
- 698 38. Shifrin N, Raulet DH, and Ardolino M. NK cell self tolerance, responsiveness and missing
699 self recognition. *Semin Immunol*. 2014;26(2):138-44.
- 700 39. Iannello A, Thompson TW, Ardolino M, Marcus A, and Raulet DH. Immunosurveillance
701 and immunotherapy of tumors by innate immune cells. *Current opinion in immunology*.
702 2015;38:52-8.
- 703 40. Benson DM, Jr., Bakan CE, Mishra A, Hofmeister CC, Efebera Y, Becknell B, et al. The
704 PD-1/PD-L1 axis modulates the natural killer cell versus multiple myeloma effect: a

- therapeutic target for CT-011, a novel monoclonal anti-PD-1 antibody. *Blood*. 2010;116(13):2286-94.
- 707 41. Beldi-Ferchiou A, Lambert M, Dogniaux S, Vely F, Vivier E, Olive D, et al. PD-1 mediates
708 functional exhaustion of activated NK cells in patients with Kaposi sarcoma. *Oncotarget*.
709 2016.
- 710 42. Pesce S, Greppi M, Tabellini G, Rampinelli F, Parolini S, Olive D, et al. Identification of a
711 subset of human natural killer cells expressing high levels of programmed death 1: A
712 phenotypic and functional characterization. *J Allergy Clin Immunol*. 2017;139(1):335-46 e3.
- 713 43. Liu Y, Cheng Y, Xu Y, Wang Z, Du X, Li C, et al. Increased expression of programmed cell
714 death protein 1 on NK cells inhibits NK-cell-mediated anti-tumor function and indicates
715 poor prognosis in digestive cancers. *Oncogene*. 2017.
- 716 44. Vari F, Arpon D, Keane C, Hertzberg MS, Talaulikar D, Jain S, et al. Immune evasion via
717 PD-1/PD-L1 on NK cells and monocyte/macrophages is more prominent in Hodgkin
718 lymphoma than DLBCL. *Blood*. 2018;131(16):1809-19.
- 719 45. Karre K, Ljunggren HG, Piontek G, and Kiessling R. Selective rejection of H-2-deficient
720 lymphoma variants suggests alternative immune defense strategy. *Nature*. 1986;319:675-8.
- 721 46. Matsumoto K, Morisaki T, Kuroki H, Kubo M, Onishi H, Nakamura K, et al. Exosomes
722 secreted from monocyte-derived dendritic cells support in vitro naive CD4+ T cell survival
723 through NF-(kappa)B activation. *Cellular immunology*. 2004;231(1-2):20-9.
- 724 47. Ardolino M, Azimi CS, Iannello A, Trevino TN, Horan L, Zhang L, et al. Cytokine therapy
725 reverses NK cell anergy in MHC-deficient tumors. *J Clin Invest*. 2014;124(11):4781-94.
- 726 48. Seaman WE, Sleisenger M, Eriksson E, and Koo GC. Depletion of natural killer cells in
727 mice by monoclonal antibody to NK-1.1. Reduction in host defense against malignancy
728 without loss of cellular or humoral immunity. *J Immunol*. 1987;138(12):4539-44.
- 729 49. Sorensen MR, Pedersen SR, Lindkvist A, Christensen JP, and Thomsen AR. Quantification
730 of B16 melanoma cells in lungs using triplex Q-PCR--a new approach to evaluate
731 melanoma cell metastasis and tumor control. *PLoS One*. 2014;9(1):e87831.
- 732 50. Castle JC, Loewer M, Boegel S, de Graaf J, Bender C, Tadmor AD, et al. Immunomic,
733 genomic and transcriptomic characterization of CT26 colorectal carcinoma. *BMC Genomics*.
734 2014;15:190.
- 735 51. Chiossone L, Chaix J, Fuseri N, Roth C, Vivier E, and Walzer T. Maturation of mouse NK
736 cells is a 4-stage developmental program. *Blood*. 2009;113(22):5488-96.
- 737 52. Joncker NT, Fernandez NC, Treiner E, Vivier E, and Raulet DH. NK cell responsiveness is
738 tuned commensurate with the number of inhibitory receptors for self-MHC class I: the
739 rheostat model. *J Immunol*. 2009;182(8):4572-80.
- 740 53. Joncker NT, Shifrin N, Delebecque F, and Raulet DH. Mature natural killer cells reset their
741 responsiveness when exposed to an altered MHC environment. *J Exp Med*.
742 2010;207(10):2065-72.
- 743 54. Elliott JM, Wahle JA, and Yokoyama WM. MHC class I-deficient natural killer cells
744 acquire a licensed phenotype after transfer into an MHC class I-sufficient environment. *J*
745 *Exp Med*. 2010;207(10):2073-9.
- 746 55. Huang AC, Postow MA, Orlowski RJ, Mick R, Bengsch B, Manne S, et al. T-cell
747 invigoration to tumour burden ratio associated with anti-PD-1 response. *Nature*.
748 2017;545(7652):60-5.
- 749 56. Martincorena I, and Campbell PJ. Somatic mutation in cancer and normal cells. *Science*.
750 2015;349(6255):1483-9.

- 751 57. Van Allen EM, Miao D, Schilling B, Shukla SA, Blank C, Zimmer L, et al. Genomic
752 correlates of response to CTLA-4 blockade in metastatic melanoma. *Science*.
753 2015;350(6257):207-11.
- 754 58. Diaz LA, Jr., and Le DT. PD-1 Blockade in Tumors with Mismatch-Repair Deficiency. *N*
755 *Engl J Med*. 2015;373(20):1979.
- 756 59. McGranahan N, Furness AJ, Rosenthal R, Ramskov S, Lyngaa R, Saini SK, et al. Clonal
757 neoantigens elicit T cell immunoreactivity and sensitivity to immune checkpoint blockade.
758 *Science*. 2016;351(6280):1463-9.
- 759 60. Garrido F, Cabrera T, Lopez-Nevot MA, and Ruiz-Cabello F. HLA class I antigens in
760 human tumors. *Adv Cancer Res*. 1995;67:155-95.
- 761 61. Raulet DH, and Guerra N. Oncogenic stress sensed by the immune system: role of natural
762 killer cell receptors. *Nat Rev Immunol*. 2009;9(8):568-80.
- 763 62. Paschen A, Baingo J, and Schadendorf D. Expression of stress ligands of the
764 immunoreceptor NKG2D in melanoma: regulation and clinical significance. *Eur J Cell Biol*.
765 2014;93(1-2):49-54.
- 766 63. Zhang J, Basher F, and Wu JD. NKG2D Ligands in Tumor Immunity: Two Sides of a Coin.
767 *Front Immunol*. 2015;6:97.
- 768 64. Fionda C, Soriani A, Zingoni A, Santoni A, and Cippitelli M. NKG2D and DNAM-1
769 Ligands: Molecular Targets for NK Cell-Mediated Immunotherapeutic Intervention in
770 Multiple Myeloma. *Biomed Res Int*. 2015;2015:178698.
- 771 65. Zingoni A, Fionda C, Borrelli C, Cippitelli M, Santoni A, and Soriani A. Natural Killer Cell
772 Response to Chemotherapy-Stressed Cancer Cells: Role in Tumor Immunosurveillance.
773 *Front Immunol*. 2017;8:1194.
- 774 66. Gordon SR, Maute RL, Dulken BW, Hutter G, George BM, McCracken MN, et al. PD-1
775 expression by tumour-associated macrophages inhibits phagocytosis and tumour immunity.
776 *Nature*. 2017;545(7655):495-9.
- 777 67. Schietinger A, Philip M, Krisnawan VE, Chiu EY, Delrow JJ, Basom RS, et al. Tumor-
778 Specific T Cell Dysfunction Is a Dynamic Antigen-Driven Differentiation Program Initiated
779 Early during Tumorigenesis. *Immunity*. 2016;45(2):389-401.
- 780 68. Legat A, Speiser DE, Pircher H, Zehn D, and Fuertes Marraco SA. Inhibitory Receptor
781 Expression Depends More Dominantly on Differentiation and Activation than "Exhaustion"
782 of Human CD8 T Cells. *Front Immunol*. 2013;4:455.
- 783 69. Terme M, Ullrich E, Aymeric L, Meinhardt K, Desbois M, Delahaye N, et al. IL-18 induces
784 PD-1-dependent immunosuppression in cancer. *Cancer Res*. 2011;71(16):5393-9.
- 785 70. Mittal D, Young A, Stannard K, Yong M, Teng MW, Allard B, et al. Antimetastatic effects
786 of blocking PD-1 and the adenosine A2A receptor. *Cancer Res*. 2014;74(14):3652-8.
- 787 71. Romagne F, Andre P, Spee P, Zahn S, Anfossi N, Gauthier L, et al. Preclinical
788 characterization of 1-7F9, a novel human anti-KIR receptor therapeutic antibody that
789 augments natural killer-mediated killing of tumor cells. *Blood*. 2009;114(13):2667-77.
- 790 72. Kohrt HE, Houot R, Weiskopf K, Goldstein MJ, Scheeren F, Czerwinski D, et al.
791 Stimulation of natural killer cells with a CD137-specific antibody enhances trastuzumab
792 efficacy in xenotransplant models of breast cancer. *J Clin Invest*. 2012;122(3):1066-75.
- 793 73. Deng W, Gowen BG, Zhang L, Wang L, Lau S, Iannello A, et al. Antitumor immunity. A
794 shed NKG2D ligand that promotes natural killer cell activation and tumor rejection. *Science*.
795 2015;348(6230):136-9.

796 74. Triebel F, Jitsukawa S, Baixeras E, Roman-Roman S, Genevee C, Viegas-Pequignot E, et al.
797 LAG-3, a novel lymphocyte activation gene closely related to CD4. *Journal of Experimental*
798 *Medicine*. 1990;171(5):1393-405.

799 75. Stojanovic A, Fiegler N, Brunner-Weinzierl M, and Cerwenka A. CTLA-4 is expressed by
800 activated mouse NK cells and inhibits NK Cell IFN-gamma production in response to
801 mature dendritic cells. *J Immunol*. 2014;192(9):4184-91.

802 76. Chan CJ, Martinet L, Gilfillan S, Souza-Fonseca-Guimaraes F, Chow MT, Town L, et al.
803 The receptors CD96 and CD226 oppose each other in the regulation of natural killer cell
804 functions. *Nat Immunol*. 2014;15(5):431-8.

805 77. Guerra N, Tan YX, Joncker NT, Choy A, Gallardo F, Xiong N, et al. NKG2D-deficient
806 mice are defective in tumor surveillance in models of spontaneous malignancy. *Immunity*.
807 2008;28(4):571-80.

808 78. Kirsch DG, Dinulescu DM, Miller JB, Grimm J, Santiago PM, Young NP, et al. A spatially
809 and temporally restricted mouse model of soft tissue sarcoma. *Nat Med*. 2007;13(8):992-7.
810

811

812 **Figure Legends:**

813 **Figure 1: Therapeutic anti-tumor effect of PD-1 or PD-L1 antibodies, dependent on NK cells.**

814 **(A)** NK, CD4 and/or CD8 T cells were depleted before s.c. injection of 10^6 RMA-S cells. Tumor
815 volumes (means \pm S.E.) are shown. The experiments depicted are representative of two performed.
816 n=4-5/group. Statistical analyses with two-way ANOVA test.

817 **(B)** PD-L1 expression was analyzed on cells stimulated or not with 20 ng/ml of IFN- γ for 48 hours.
818 Representative of 3 performed.

819 **(C)** 2×10^6 RMA-S or RMA-S-*Pdl1* cells (naturally expressing CD45.2) or TRAMP-C2 cells
820 (transduced with Thy1.1) were injected s.c. into C57BL/6-CD45.1⁺ mice, and PD-L1 expression
821 was analyzed on splenic or intratumoral cells, gating on dendritic cells (viable-CD45.1⁺CD3⁺CD19⁻
822 Ter119⁻NK1.1⁻CD11b⁺Ly6G⁻CD11c^{high}), monocytes (viable-CD45.1⁺CD3⁺CD19⁻Ter119⁻NK1.1⁻
823 CD11b⁺Ly6G⁻CD11c⁺Ly6C⁺), and tumor cells (viable-CD45.1⁺CD45.2⁺ cells for RMA-S and RMA-S-
824 *Pdl1*, or viable-CD45.2⁺Thy1.1⁺ for TRAMP-C2). The MFI of isotype control-stained cells was
825 subtracted from the MFI of PD-L1-stained cells. Two experiments were pooled (n=5-7/group).

826 **(D)** 10^6 RMA-S-*Pdl1* cells were injected in mice depleted of NK, CD8 or CD4 T cells. Tumor

827 volumes (means±S.E.) are shown. Representative of two performed. n=4-5/group. Statistical
828 analyses with two-way ANOVA test.

829 **(E)** 10^6 RMA-S-*Pdl1* cells were injected in C57BL/6 mice and after two days 250 µg of PD-1 or
830 control antibody were administered. Some mice were depleted of NK cells two days before tumor
831 cell injection. In the figure, we pooled data from 2 of the 3 experiments performed, n=6-11/group.
832 Statistical analyses with two-way ANOVA tests. Both NK-depleted groups were significantly
833 different than the corresponding undepleted groups.

834 **(F)** 10^6 RMA-S-*Pdl1* cells were injected and tumors were allowed to grow to an average of 25 mm³,
835 at which time (and two days later) the mice were treated with 250 µg of PD-1 antibody or clg.
836 Representative of 2 performed, n=5/group. Statistical analyses with two-way ANOVA tests.

837 **(G-H)** 0.5×10^6 RMA-S-*Pdl1* tumor cells were mixed with Matrigel and either 20 µg of anti-PD-1 or
838 control Ig **(E, G)** or anti-PD-L1 or control Ig **(F, H)** and injected s.c.. in C57BL/6 mice. Experiments
839 were repeated at least two times, with n=4-5/group. Statistical analyses with two-way ANOVA
840 tests.

841
842 **Figure 2: PD-1 is expressed on tumor infiltrating NK cells and suppresses NK cell**
843 **cytotoxicity in vitro.**

844 **(A-B)** C57BL/6 mice were injected s.c. with 2×10^6 RMA-S cells or PBS; BALB/cJ mice were
845 injected with 0.5×10^6 CT26 cells. PD-1 expression was assessed after 13 days on NK cells from
846 spleens, axillary lymph nodes, inguinal lymph nodes and tumors. Staining for PD-1 (dark-grey filled
847 histograms) or control IgG (light-grey filled histograms) is shown. NK cells were gated as viable-
848 Ter119-CD3-CD19-F4/80-NKp46⁺ cells in BALB/cJ, or Ter119-CD3-CD19-F4/80-NKp46⁺NK1.1⁺ cells
849 in C57BL/6 mice. Representative of six experiments performed with n=3-5.

850 **(C)** Summary of PD-1 expression on intratumoral NK and CD8⁺ T cells in mice injected with RMA,
851 RMA-S, B16, C1498, CT26, 4T1 or A20 cells, or on intratumoral NK cells in the prostates or thymi

852 from spontaneous cancer models (TRAMP and Eu-Myc models, respectively), or in KP sarcomas.
853 PD-1 expression on NK cells in each model was assessed in at least 3 independent experiments,
854 with at least n=3.

855 **(D-E)** IL-2-activated NK cells previously transduced with a *Pdcd1* expression vector were
856 stimulated with RMA-S or RMA-S-*Pdl1* cells at different target to effector (T:E) ratios before
857 determining degranulation **(D)** and IFN- γ production **(E)** of PD-1⁺ NK cells. The experiments
858 depicted are representative of 3 performed. Every T:E ratio is the average \pm S.D. of 3 technical
859 replicates. Statistical analysis employed two-way ANOVA.

860 **(F-G)** NK92 cells transduced with *Pdcd1* (*Pdcd1* encodes PD-1) or an empty vector, were
861 stimulated with K562 or K562-*Pdl1* cells and lysis of target cells **(F)** or degranulation of effector
862 cells **(G)** was assessed by flow cytometry. F and G are representative of 4 and 2 experiments
863 performed, respectively. Every T:E ratio is the average of 3 technical replicates. Statistical analysis
864 employed two-way ANOVA with repeated measures.

865
866 **Figure 3: Expression of PD-L1 by NK cell-sensitive, T cell-resistant tumor cells promotes**
867 **more aggressive tumor growth in vivo.**

868 **(A)** RMA-S cells were transduced with a PD-L1 expression or an empty control vector. G418-
869 resistant transductants were selected. Transduced cells, as well as untransduced RMA-S cells,
870 were injected in C57BL/6 mice (10⁶ cells/mouse s.c.) and tumor growth was monitored. Tumor
871 volumes (means \pm S.E.) are shown for each time-point. The experiment shown is representative of
872 3 performed, n=5-6. Statistical analyses with two-way ANOVA (*: p<0.05).

873 Survival **(B)** and in vivo tumor growth (means \pm SE) **(C)** were assessed after s.c. injection of 1x10⁶
874 RMA-S or RMA-S-*Pdl1* tumor cells in C57BL/6 mice. Where indicated, NK cells were depleted by
875 injecting NK1.1 antibody. The results depicted were representative of 8 independent experiments,

876 two of which included NK cell-depleted mice for comparison. In the experiment shown, n=6-7 per
877 group. Statistical analyses were performed in A with the log-rank (Mantel-Cox) test and in B with a
878 two-way ANOVA test (**: $p < 0.01$).

879 **(D)** 10^6 RMA-S or RMA-S-*Pd11* cells were injected s.c. into *Rag1^{-/-}Il2rg^{-/-}* mice, and tumor growth
880 was assessed. Tumor volumes (means \pm S.E.) are shown. The experiment shown is representative
881 of 3 independent experiments, n=4/group.

882 **(E)** 10^6 RMA or RMA-*Pd11* tumor cells were injected s.c. into C57BL/6 mice and tumor growth was
883 monitored. Tumor volumes (means \pm S.E.) are shown. The experiment shown is representative of
884 two performed. n=5 for RMA group and 6 for RMA-*Pd11* group.

885

886 **Figure 4: PD-1 suppresses NK cell-mediated control of B16 colonization in the lungs.**

887 **(A)** B16-BL6 cells were transduced with a retroviral vector encoding mouse PD-L1, and sorted for
888 PD-L1 expression, which is depicted.

889 **(B)** C57BL/6 mice were injected i.v. with 0.25×10^6 B16-BL6 tumor cells or saline solution. When
890 mice were terminally ill, PD-1 expression was assessed by flow cytometry on splenic or lung NK
891 cells. NK cells were gated as viable-CD45⁺Ter119⁻CD3⁻CD19⁻F4/80⁻NK1.1⁺NKp46⁺. In E: n=3 for
892 the control group and 11 for B16 group. Statistical analyses with a Student's t-test.

893 **(C-F)** Kaplan-Meier analyses of C57BL/6 mice injected i.v. with 5,000 (C-D) or 20,000 (E-F) B16 or
894 B16-*Pd11* cells. In D and F, mice were NK-depleted with NK1.1 antibody. C and D represent results
895 pooled from 2 experiments, with n=7-15/group. E and F: results pooled from 2 experiments, with
896 n=8-12/combined group. Statistical analyses with the log-rank (Mantel-Cox) test.

897 **(G)** C57BL/6 mice were injected i.v. with 2×10^4 B16 or B16-*Pd11* cells. 21 days later, the presence
898 of tumors in the lungs was assessed by macroscopic examination. Data from the combination of
899 two independent experiments with n=12-13/ combined group; statistical analysis with Fisher's
900 exact test.

901 **(H)** C57BL/6 mice were injected i.v. with 20,000 B16 or B16-*Pdl1* cells. 21 days later, tumors
902 burden in the lungs was assessed by q-RT-PCR of transcripts of the melanoma-specific gene
903 *Gp100*. H is the combination of two independent experiments with n=9-10/group; statistical
904 analysis with Mann-Whitney test.

905
906 **Figure 5: PD-L1 expression by CT26 tumor cells prevents tumor rejection mediated by NK**
907 **cells and CD8 T cells.**

908 **(A)** PD-L1 expression by CT26 cell variants. Cells were untreated or treated with 20 ng/ml of IFN- γ
909 for 48 hrs and PD-L1 expression was analyzed by flow cytometry. Top panel: Comparison of CT26
910 and CT26-*Pdl1*^{-/-} cells. Lower panel: Comparison of CT26-*Pdl1*^{-/-} cells transduced with a PD-L1
911 expression vector or with an empty vector. Wildtype CT26 cells transduced with empty vector
912 served as a control.

913 **(B, C)** In vivo growth of CT26 or CT26-*Pdl1*^{-/-} tumors was assessed after s.c. injection of 0.5×10^6
914 cells in BALB/cJ mice. Some mice were depleted of NK cells (with asialoGM-1 antibody), CD8 T
915 cells (with CD8 α -specific 2.43 antibody), or both, before tumor cell injection. Tumor volumes
916 (means \pm S.E.) are shown. In panel B: two-way ANOVA tests were used to compare CT26-*Pdl1*^{-/-}
917 /undepleted mice to either CT26/undepleted mice ($p < 0.01$), CT26-*Pdl1*^{-/-}/NK-depleted mice
918 ($p < 0.0001$), or CT26-*Pdl1*^{-/-}/CD8-depleted mice ($p < 0.01$). Two-way ANOVA tests were also used to
919 compare CT26-*Pdl1*^{-/-}/NK&CD8-depleted mice to either CT26-*Pdl1*^{-/-} /CD8-depleted mice ($p < 0.05$)
920 or CT26-*Pdl1*^{-/-}/NK-depleted mice ($p = 0.0599$). In panel C, none of the differences were significant.
921 Data from B and C are from the same experiment, which is representative of 2 performed. n=8 for
922 the experiment shown.

923 **(D)** 0.2×10^6 CT26-*Pdl1*^{-/-} cells transduced with an empty vector or a PD-L1 expression vector, or
924 CT26 wild type cells transduced with an empty vector, were injected s.c. in BALB/cJ mice and

925 tumor progression was assessed. The experiment depicted is representative of 3 performed, n=3-4
926 mice/group. Statistical analyses with two-way ANOVA tests (*: $p < 0.05$ and ***: $p < 0.001$).

927
928 **Figure 6: NK cells are necessary to mediate full therapeutic efficacy of PD-L1 blockade in**
929 **the T cell-sensitive CT26 tumor model.**

930 **(A)** Mice were injected with 0.2×10^6 CT26-*Pdl1*^{-/-} cells transduced with an empty vector or a PD-L1
931 expression vector and treated with 250 μ g of anti-PD-L1 or control Ig daily for 10 days by i.p.
932 injection. Statistical analyses with two-way ANOVA tests (*: $p < 0.05$ and **: $p < 0.01$). n=4-5
933 mice/group. Representative of 3 performed.

934 **(B)** 0.2×10^6 CT26-*Pdl1*^{-/-} cells transduced with a PD-L1 expression vector were injected in
935 BALB/cJ mice. Where indicated, NK or CD8 T cells were depleted by i.p. injection of anti-
936 asialoGM1 or 2.43 antibodies two and one days before tumor injection. Mice were treated with 250
937 μ g of anti-PD-L1 or control Ig daily for 10 days by i.p. injection. n=4-5 mice/group. Representative
938 of 3 performed. Statistical analyses with Mann-Whitney tests comparing the anti-PD-L1 group with
939 the other experimental groups at days 15, 17 and 19 (*: $p < 0.05$ for all such comparisons).

940 **(C)** BALB/cJ mice were injected 0.25×10^6 CT26-*Pdl1*^{-/-} +*Pdl1* cells. PD-L1 or clg antibodies were
941 injected 3, 4, 5, 7 and 12 days after tumor injection. Some mice were NK-depleted 2, 9 and 16
942 days after tumor injection. n=6-9 mice/group. Data from the combination of two independent
943 experiments. Statistical analysis with Two-way ANOVA with repeated measurements. **: $p < 0.01$.

944 **(D)** 500,000 cells comprising a 1:1 mixture of CT26-*Pdl1*^{-/-} +*Pdl1*-*IRES*-*Thy1.1* and CT26-*Pdl1*^{-/-}
945 +*empty*-*IRES*-*Thy1.1* cells were injected in BALB/cJ mice depleted or not of NK cells. Tumors were
946 analyzed by flow cytometry as soon as they become palpable. Tumor cells were identified as
947 CD45-*Thy1.1*⁺. Representative of 3 performed, n=3/group, statistical analysis with two tailed
948 paired Student's t-test.

949 **(E)** 0.2×10^6 CT26 or CT26-*Pdl1*^{-/-} cells were injected s.c. in BALB/cJ mice. Once tumors were
950 established, mice were treated with 250 μ g/day of PD-L1 or control antibody for 2 days and
951 intracellular granzyme B expression was assessed in PD-1⁺ or PD-1-negative tumor-infiltrating NK
952 cells. Representative of 2 performed. n=3-5 mice/group. Statistical analysis with two-tailed
953 unpaired Student's t-tests, *: p<0.05.

954

955 **Figure 7: PD-1 engagement suppresses NK cell responses to 4T1 orthotopic tumors.**

956 **(A)** 4T1 or 4T1-*Pdl1*^{-/-} cells were stimulated or not with IFN- γ and PD-L1 expression was analyzed
957 by flow cytometry.

958 **(B-E)** 100,000 tumor cells were injected in the mammary fat pad of BALB/cJ mice. Where
959 indicated, mice were immune-depleted two and one days before tumor injection, and then 7 and 14
960 days after tumor injection. Results from B and C come from the same experiment. Results from D
961 and E come from the same experiment. n=7-8 mice/group. The two experiments are representative
962 of 3 performed. Statistical analysis with two-way ANOVA with repeated measurements comparing
963 every group with 4T1-*Pdl1*^{-/-} undepleted (in B and D) or with 4T1 undepleted (in C and E). *:
964 p<0.05; **: p<0.01; ****: p<0.00001.

965

966 **Figure 8: PD-1 is upregulated on the most activated tumor infiltrating NK cells.**

967 **(A)** PD-1 expression on different NK cell maturation subsets in RMA-S tumors. R0-R3 stages as
968 follows: R0=CD27⁻CD11b⁻; R1=CD27⁺CD11b⁻; R2=CD27⁺CD11b⁺; R3=CD27⁻CD11b⁺. 3
969 independent experiments were pooled (n=7-18/combined group). Statistical analysis with one-way
970 ANOVA with repeated measures.

971 **(B)** NK cells from RMA-S tumors were stained with antibodies for Ly49I, Ly49C, and NKG2A and
972 PD-1 expression was assessed on the three populations by flow cytometry. C⁺I⁺N⁺ cells expressed

973 all the receptors; C⁺ I⁺ N⁺ cells expressed at least one of the receptors; C⁻ I⁻ N⁻ NK cells lacked
974 expression of all three receptors. Data from 2 independent experiments are included. Statistical
975 analysis with one-way ANOVA with repeated measures.

976 NK cells from RMA-S (C), CT26 (D) or KP Sarcoma (E) tumors were co-stained with PD-1
977 antibody and antibody against Sca-1 or CD69. PD-1 expression was assessed by flow cytometry
978 on gated NK cells that did, or did not, express such markers. Representative contour plots and
979 summary of the data are depicted. In C and E, 3 independent experiments were pooled; in D, 2
980 independent experiments were pooled; n=6-15. Statistical analysis with two tailed paired Student's
981 t-tests.

982
983 **Figure 9: In RMA-S tumors PD-1⁺ NK cells are more functionally responsive than PD-1-**
984 **negative NK cells.**

985 NK cells from RMA-S-*Pdl1* (A) or RMA-S (B) derived tumors were stimulated with plate-bound
986 isotype control, anti-NKp46 or anti-NKR-P1C, and degranulation and IFN- γ accumulation of PD-1⁺
987 vs. PD-1⁻ NK cells was assessed. Representative of two experiments performed. n=4-5. Statistical
988 analyses with two-tailed paired Student's t-tests.

989
990 **Figure 10: In CT26 tumors PD-1⁺ NK cells are more responsive than PD-1-negative NK cells.**

991 NK cells from tumors deriving from CT26-*Pdl1*^{-/-} cells reconstituted with PD-L1 (A) or an empty
992 vector (B) were stimulated with plate-bound isotype control or anti-NKp46 or PMA/I. Degranulation
993 and IFN- γ accumulation of PD-1⁺ vs. PD-1⁻ NK cells were assessed. Representative of two
994 experiments performed. n=4. Statistical analyses with two-tailed paired Student's t-tests.

995
996 **Supplementary Figure 1: In vivo establishment of B16 tumors is delayed by NK cells but not**

997 **CD8 T cells.**

998 Kaplan-Meier analyses of C57BL/6 mice injected i.v. with 20,000 B16 or B16-*Pdl1* cells. Some
999 mice were depleted of CD8 and NK cells. n=4-5/group.

1000

1001 **Supplementary Figure 2: Expression of NK-activating ligands on tumor cell lines.**

1002 CT26, 4T1, RMA-S and B16 cells were stained with control isotypes (red histograms) or antibodies
1003 specific for H60, MULT1, pan-RAE-1, PVR or Nectin-2 (blue lines). Data are representative of two
1004 experiments performed with similar outcomes.

1005

1006 **Supplementary Figure 3: Engagement of activating receptors by tumor cells does not**
1007 **induce higher PD-1 expression on tumor-infiltrating NK cells.**

1008 **(A)** NK cells from RMA or RMA-*m157* s.c. tumors were stained for Ly49H and PD-1, and PD-1
1009 expression was analyzed on Ly49H⁺ NK cells. **(B)** NK cells from RMA-RAE-1 s.c. tumors in
1010 wildtype mice or *Klrk1*^{-/-} mice (lacking expression of NKG2D) were stained with PD-1 antibody. A is
1011 representative of two experiments performed. In B, two experiments were combined. In A,
1012 n=5/group; in B, n=11/group. In A, statistical analyses with two-tailed unpaired Student's t-tests; in
1013 B with Mann-Whitney test.

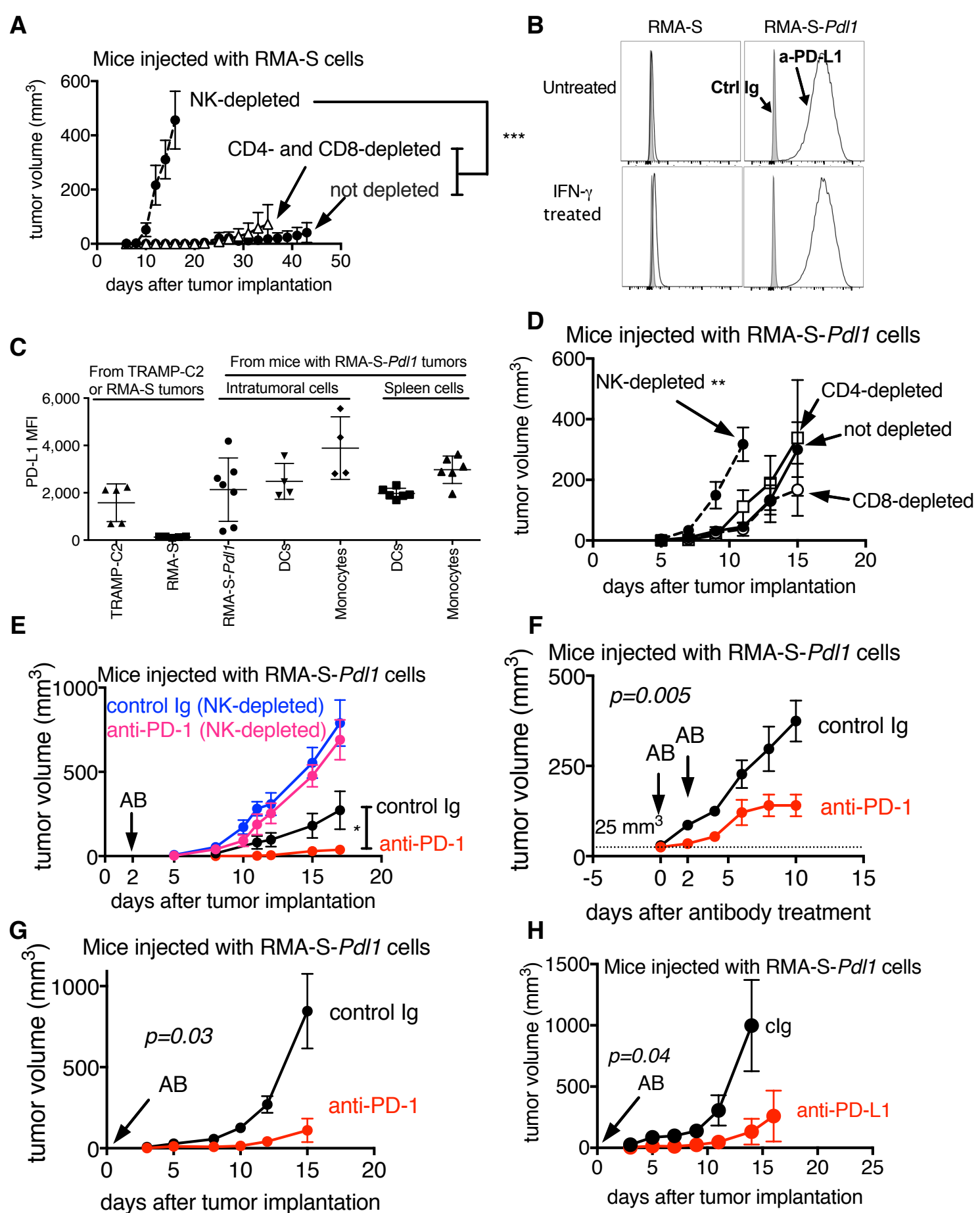
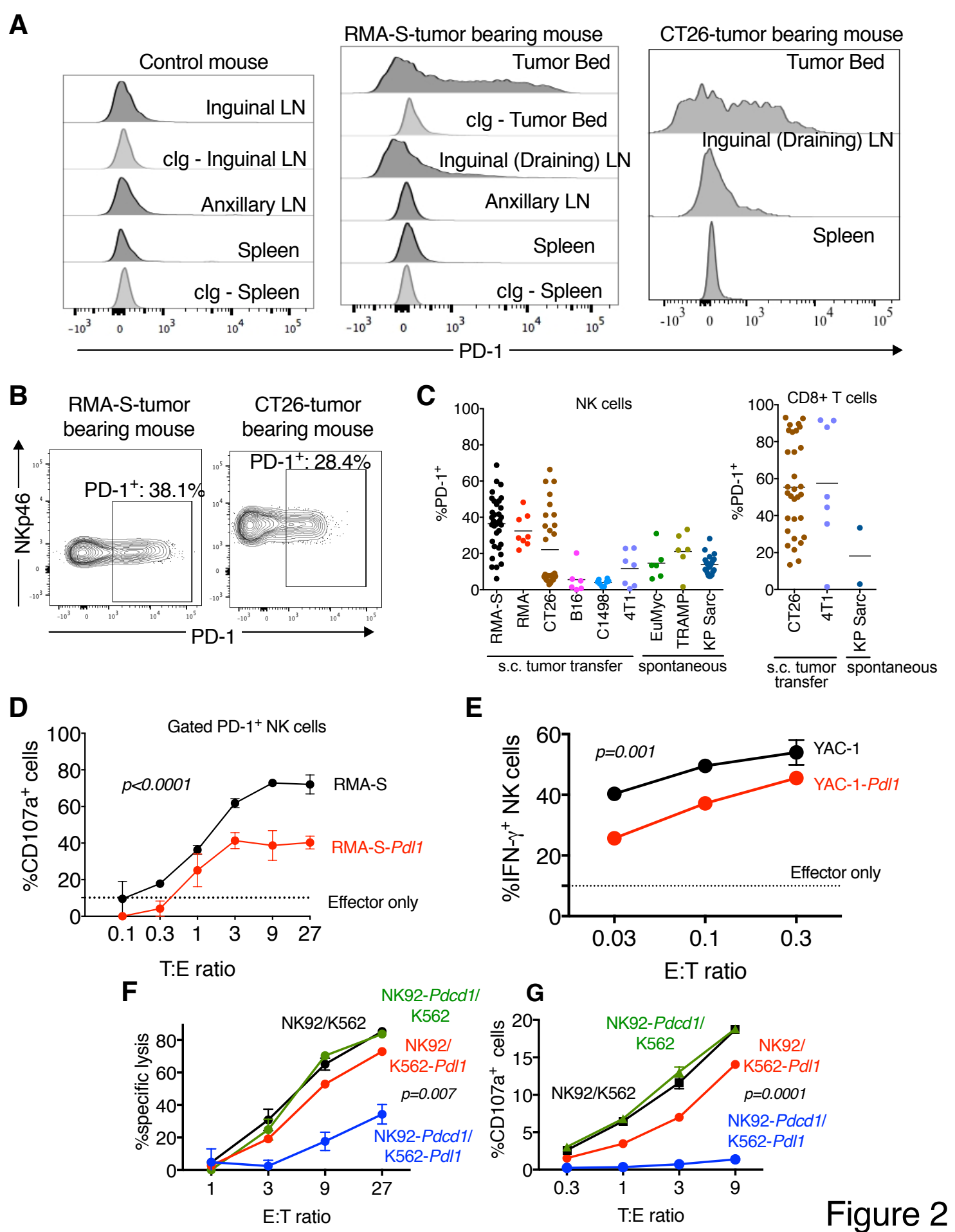


Figure 1



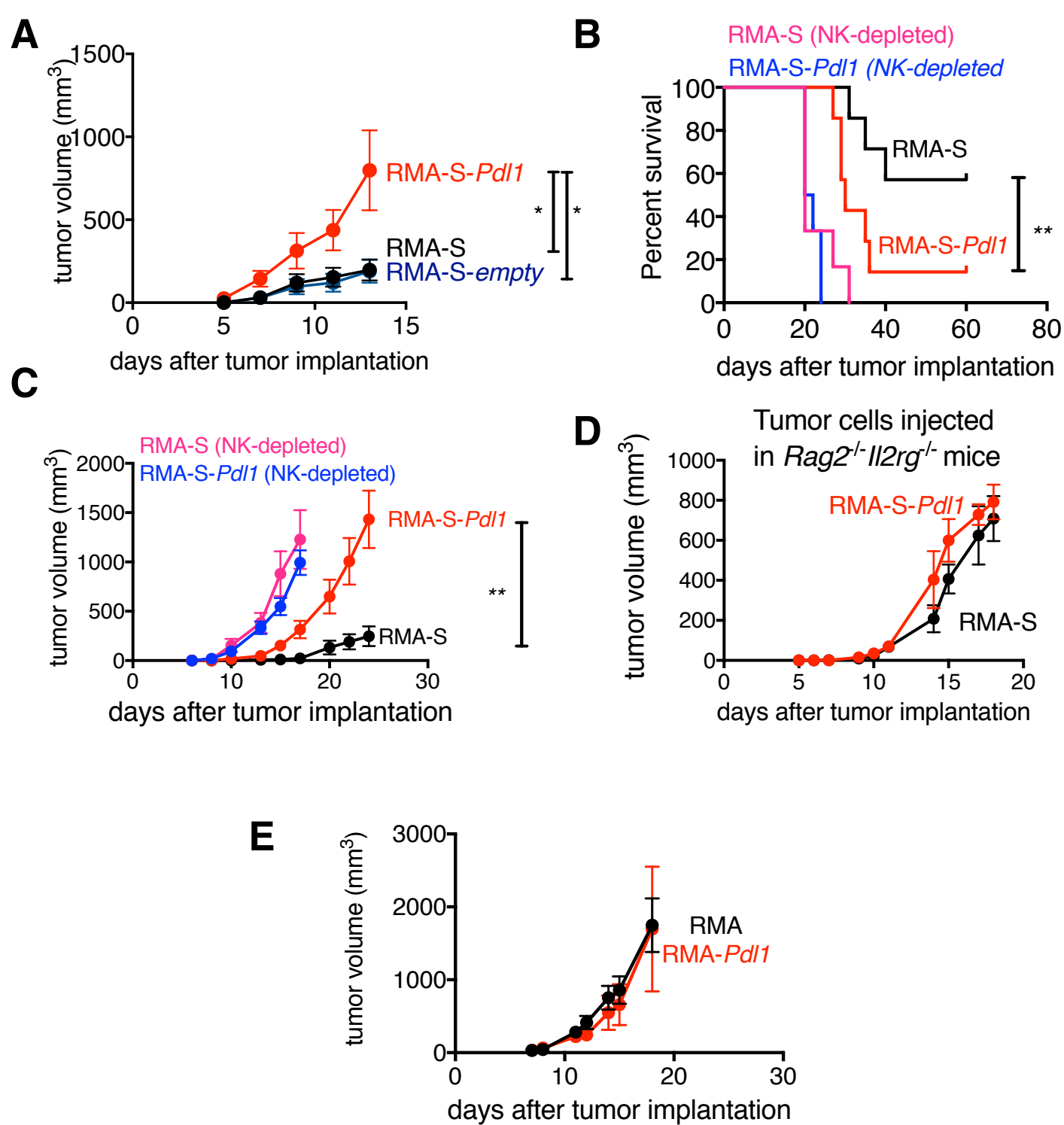


Figure 3

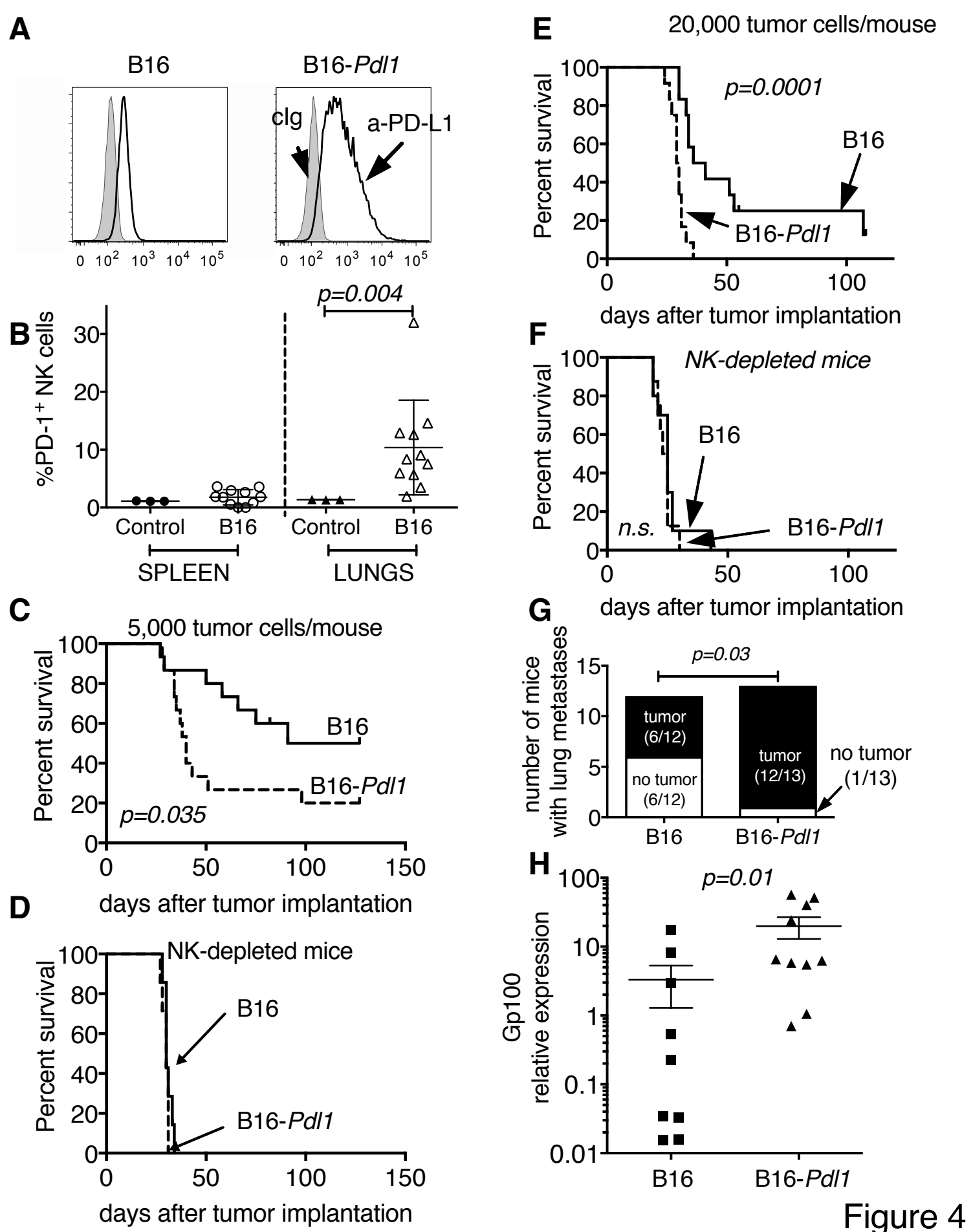


Figure 4

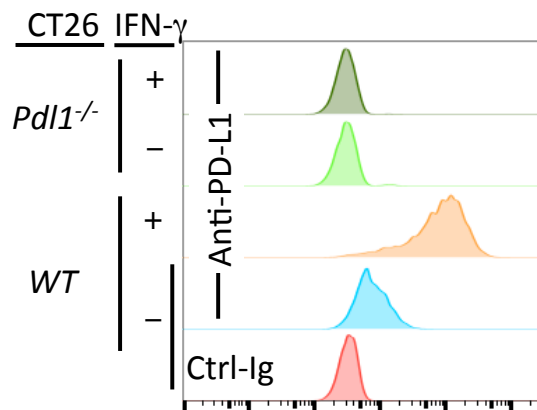
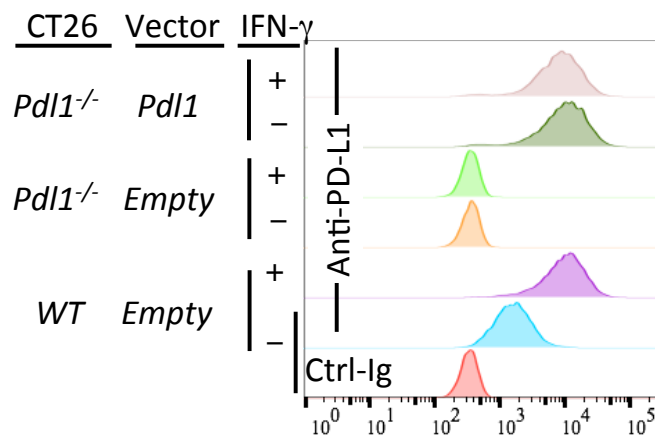
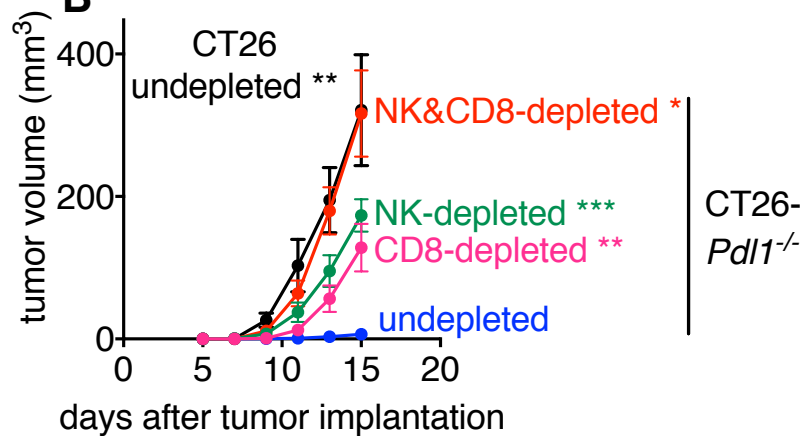
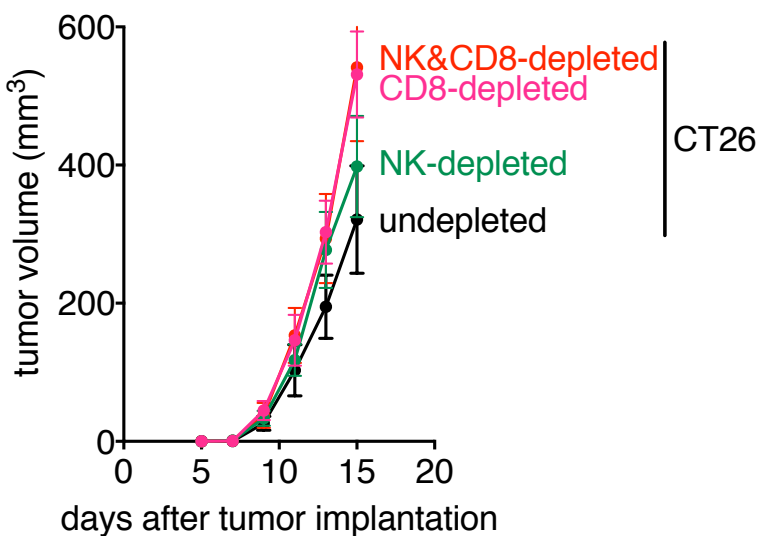
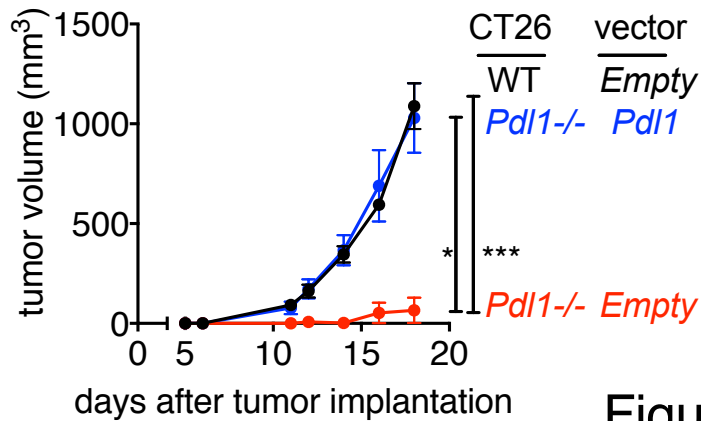
A**B****C****D**

Figure 5

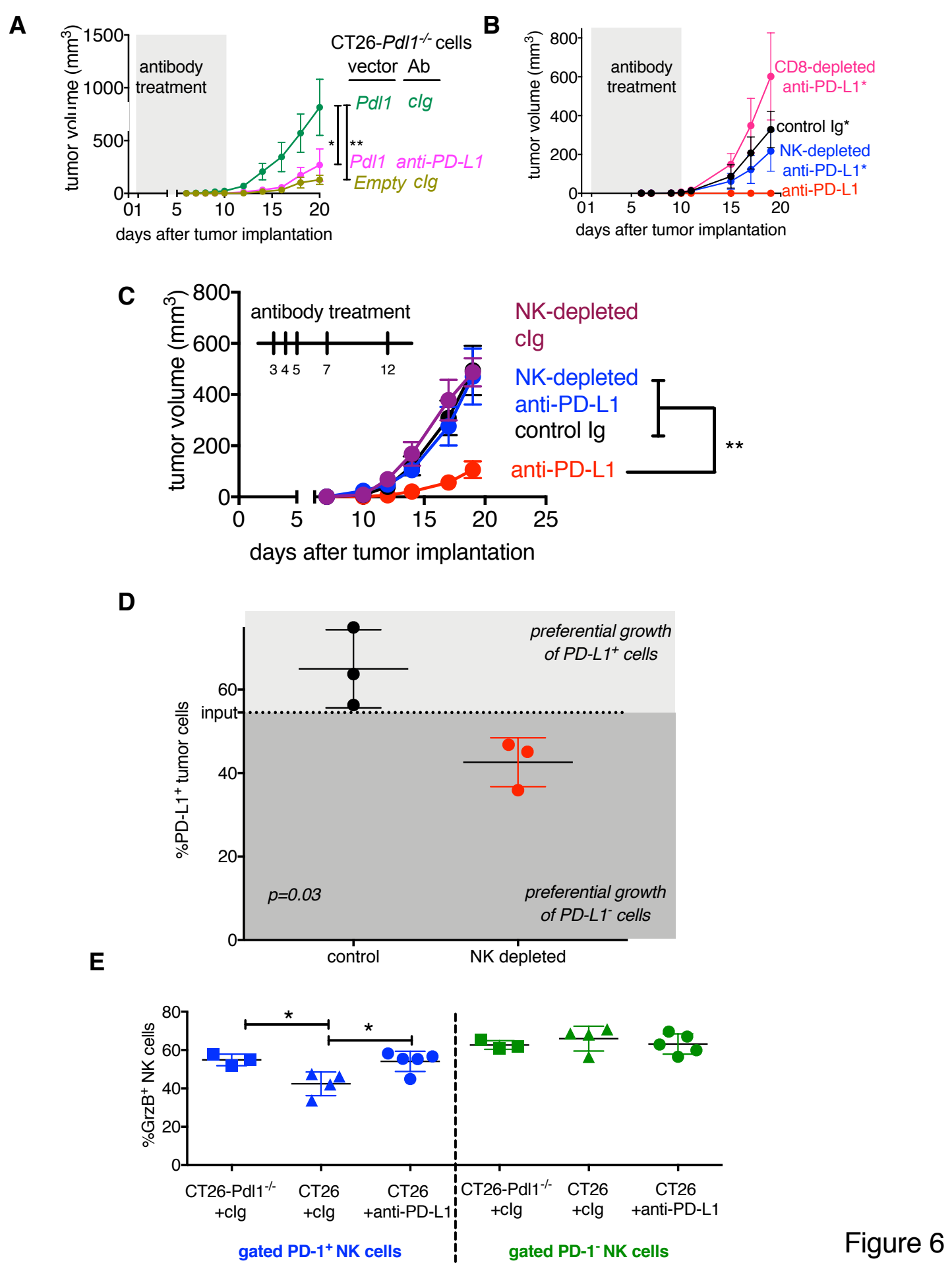


Figure 6

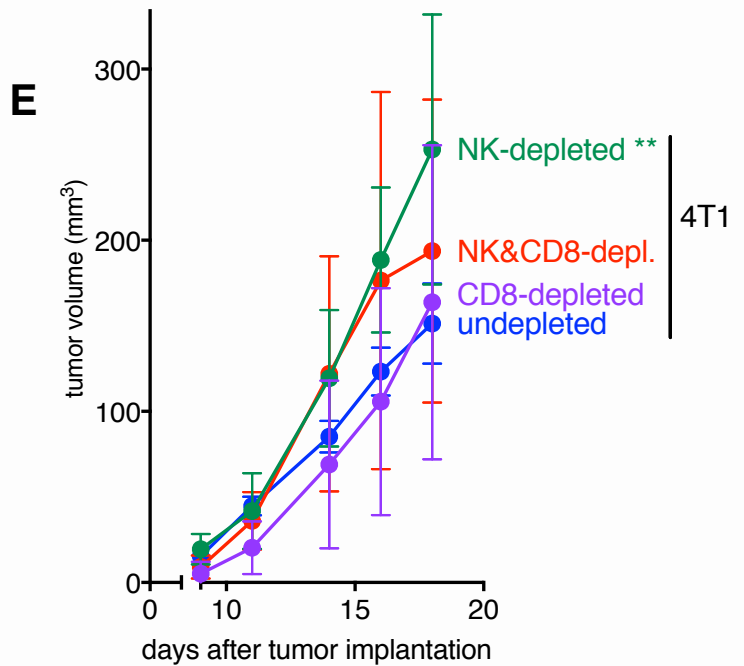
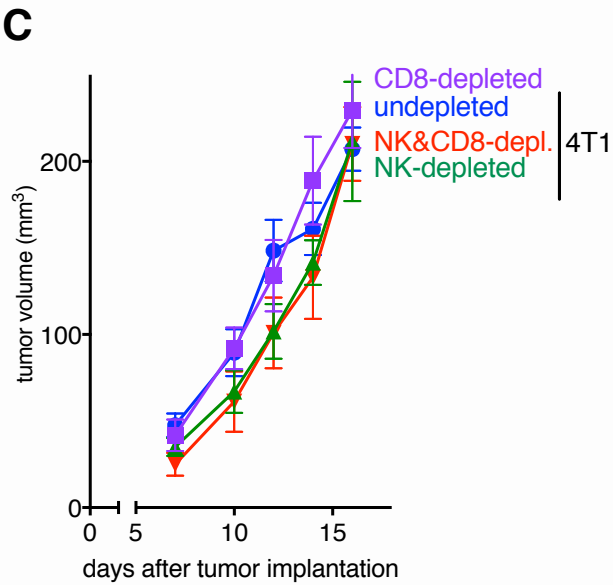
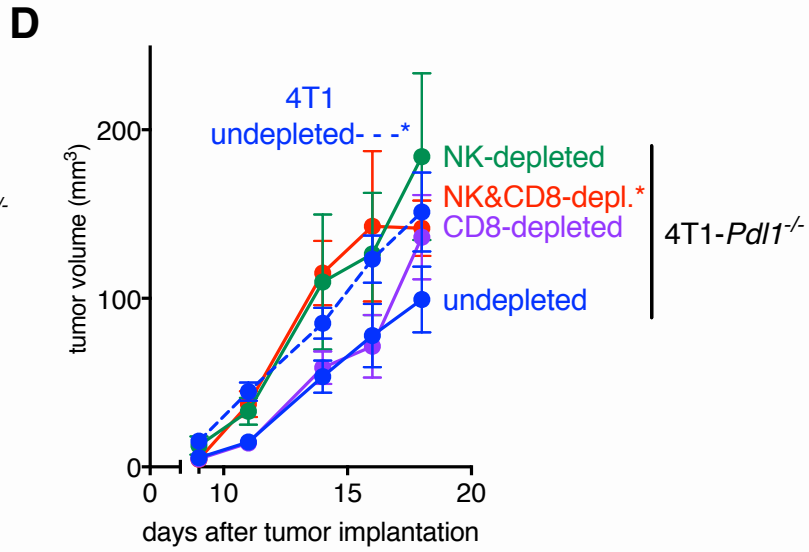
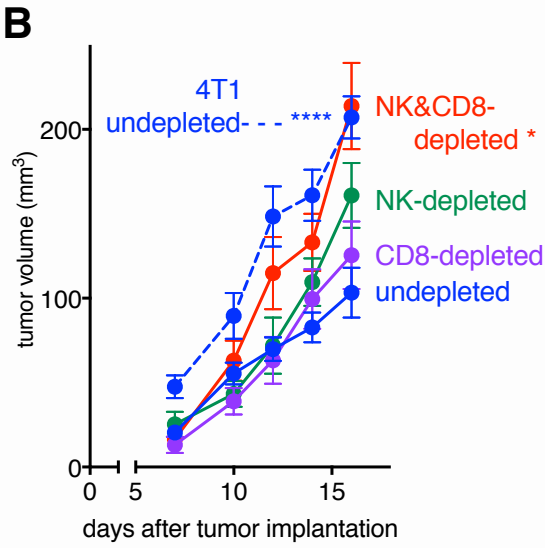
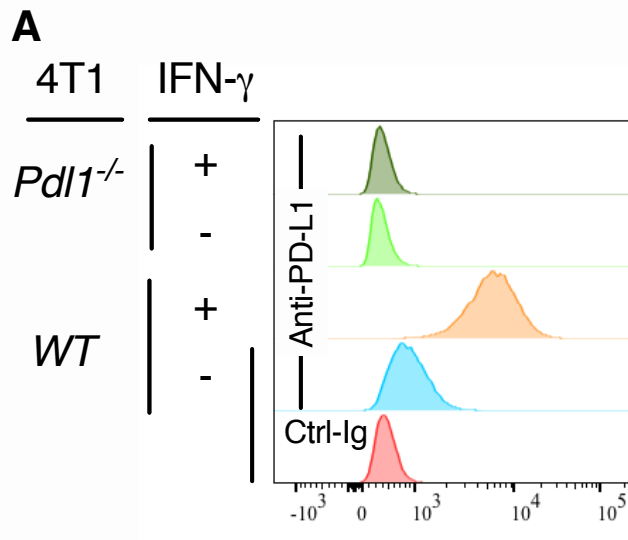
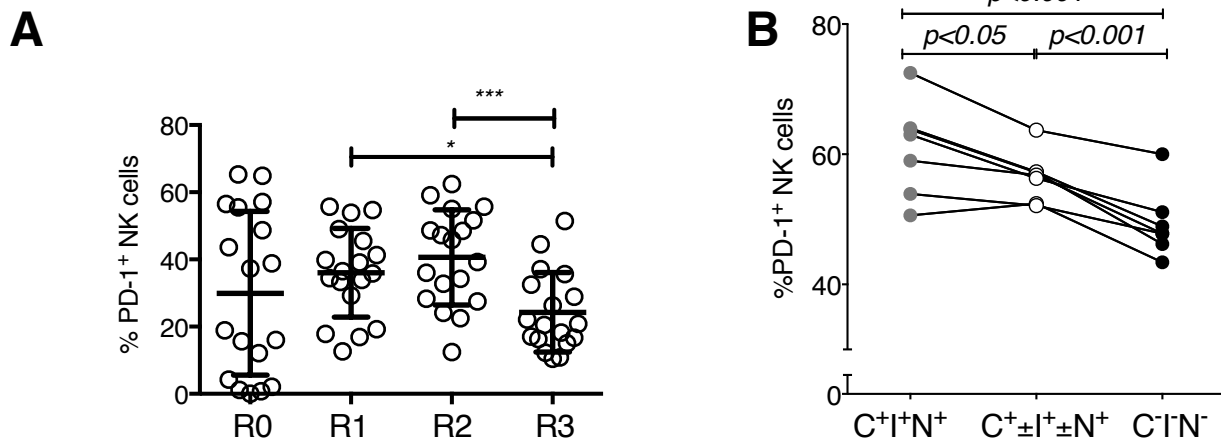
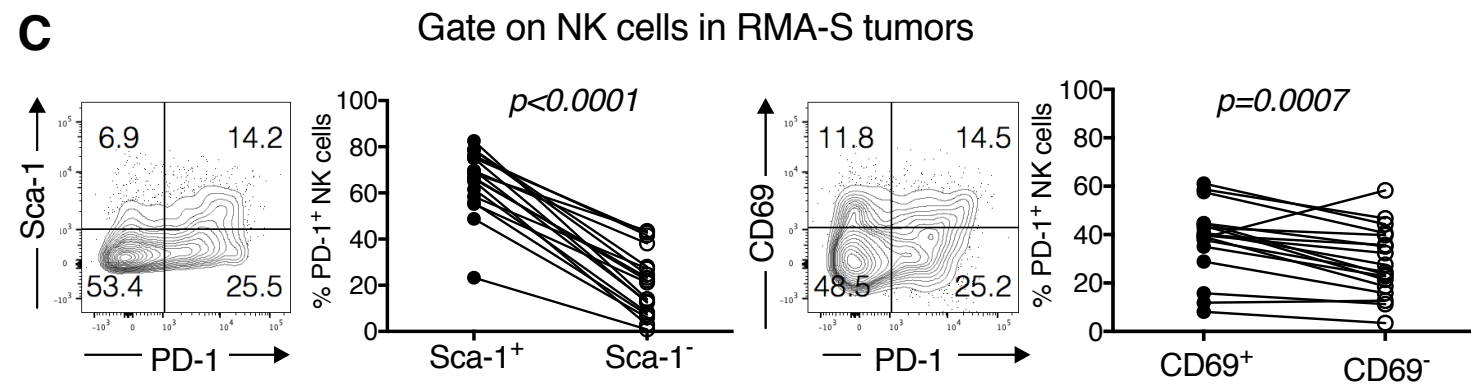


Figure 7

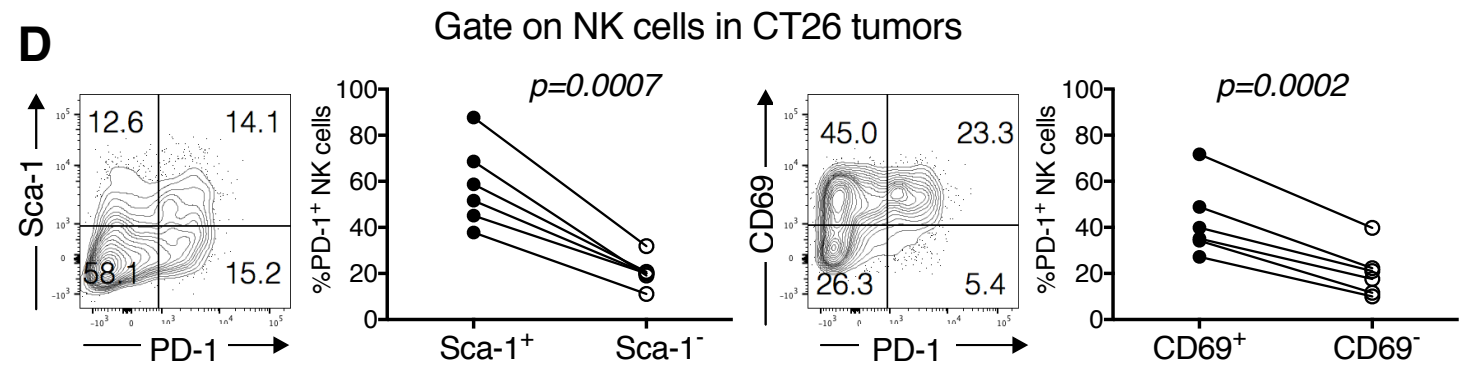
Gate on NK cells in RMA-S tumors



Gate on NK cells in RMA-S tumors



Gate on NK cells in CT26 tumors



Gate on NK cells in KP Sarcomas

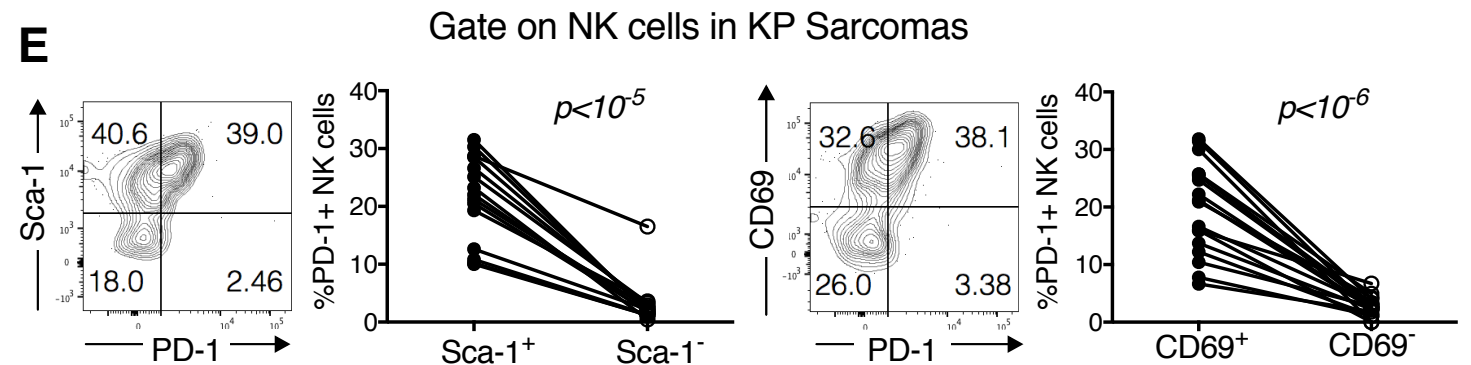
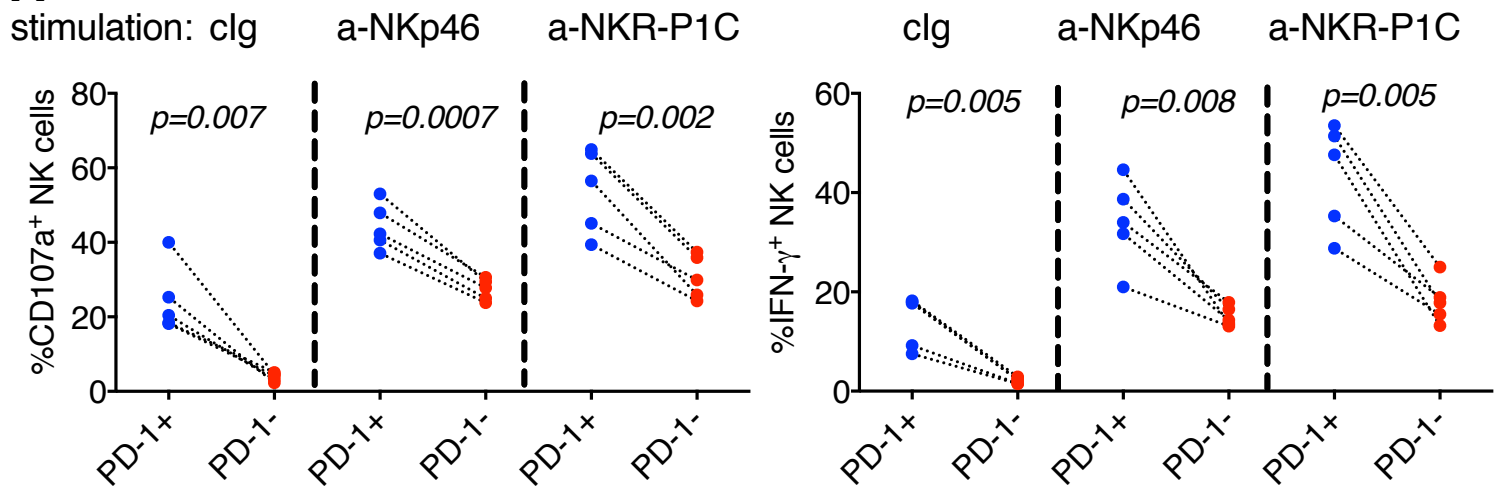


Figure 8

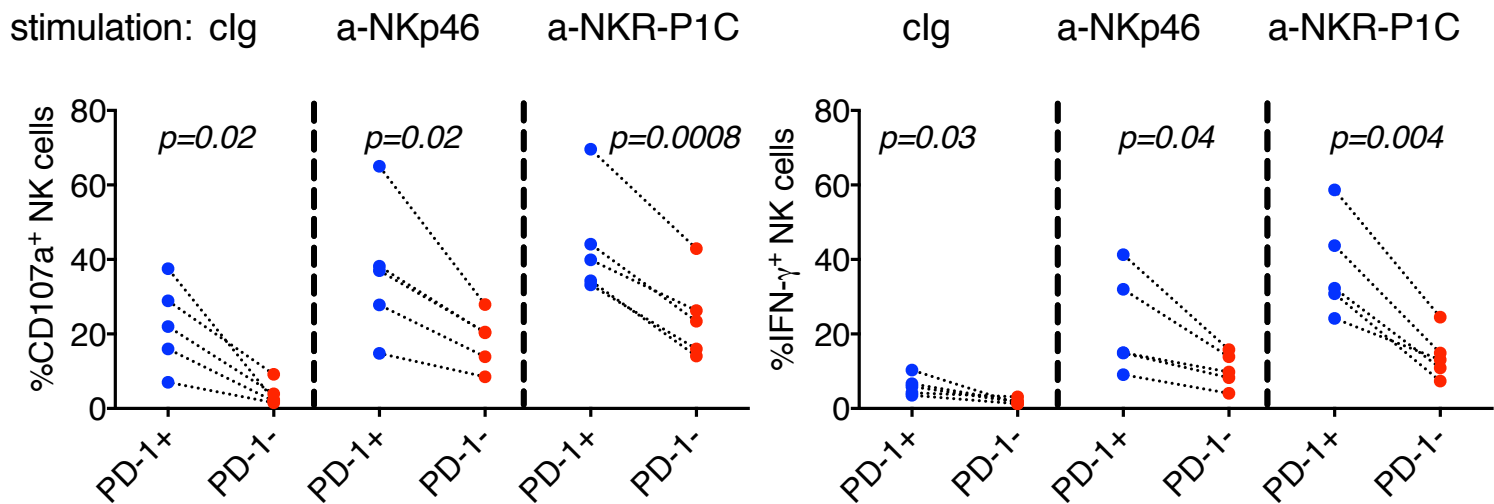
NK cells in RMA-S-*Pdl1* tumors

A

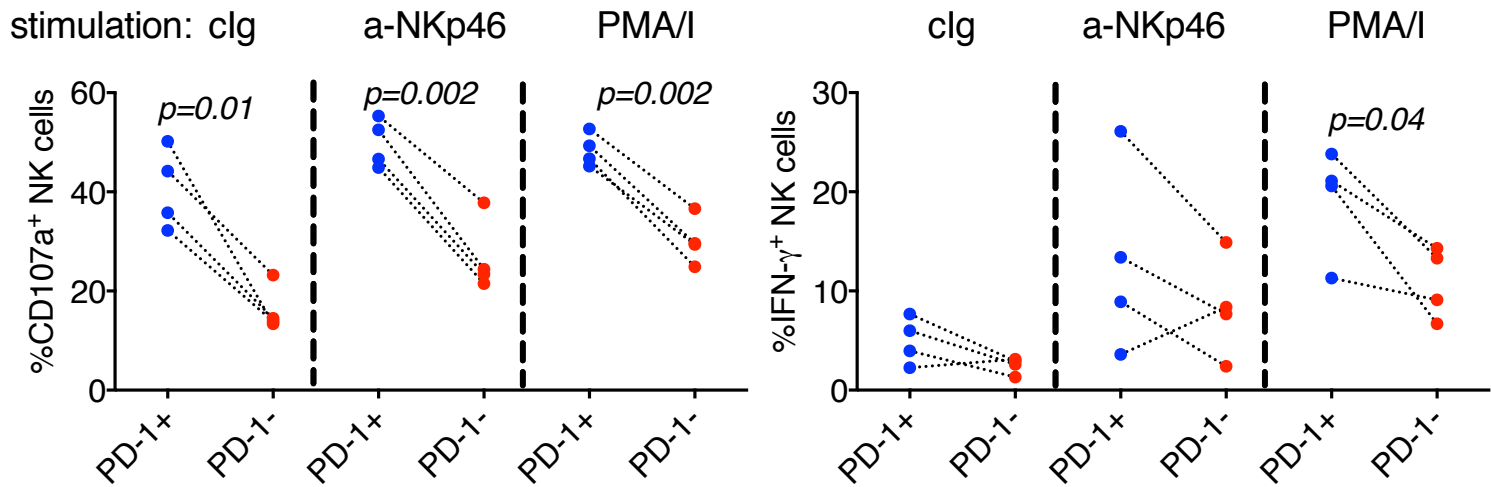


B

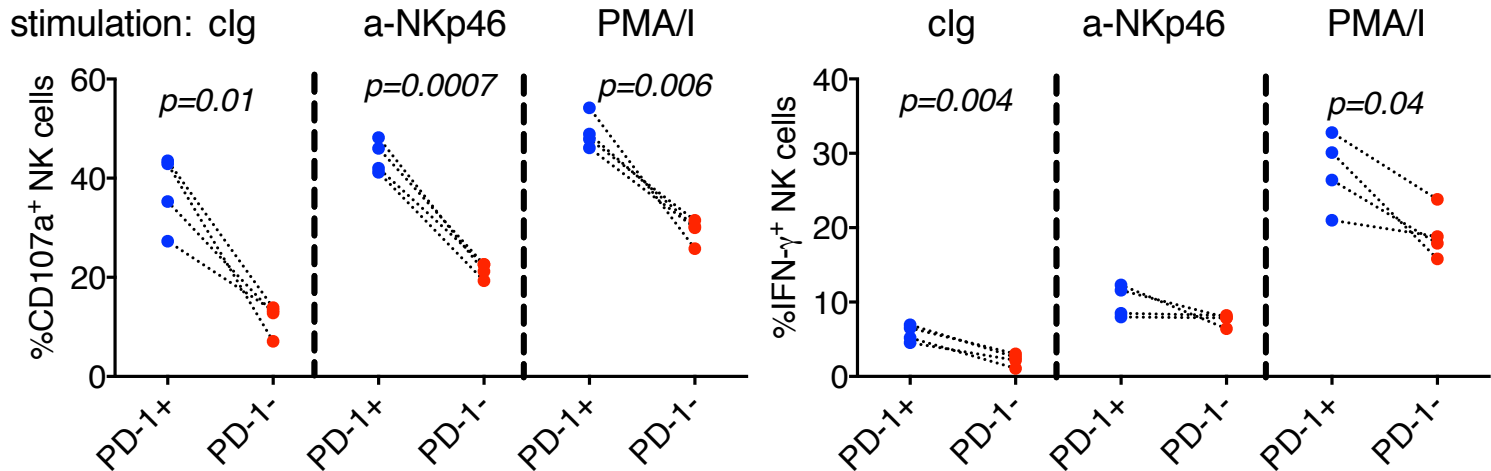
NK cells in RMA-S tumors



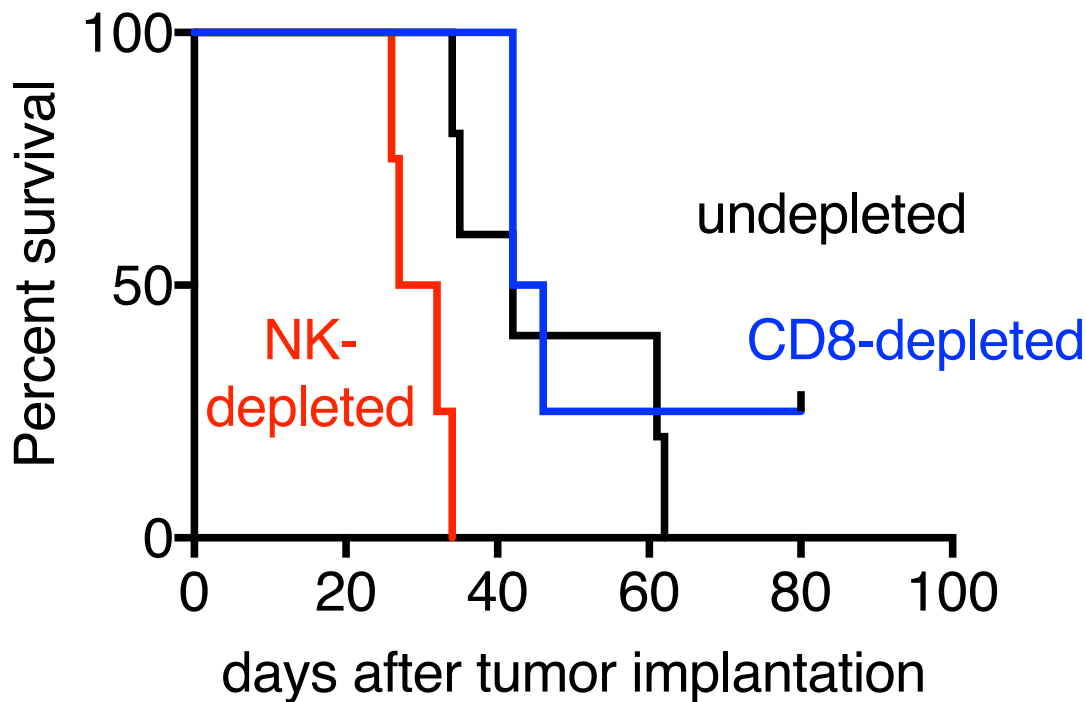
NK cells in CT26/*Pdl1*^{-/-} + PD-L1 tumors



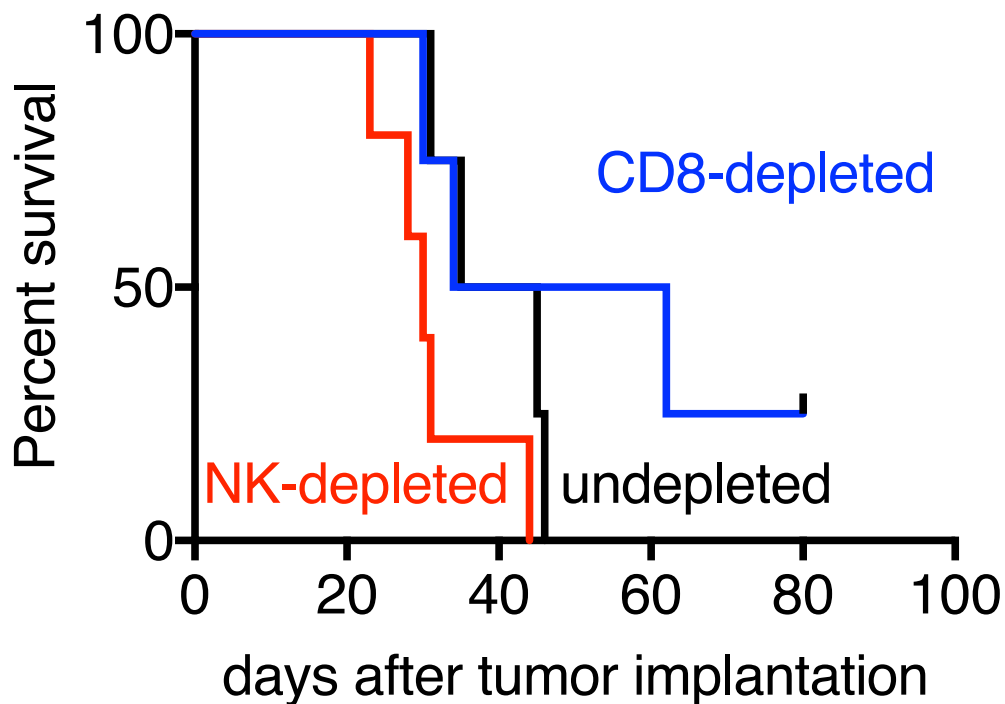
NK cells in CT26/*Pdl1*^{-/-} + empty vector tumors



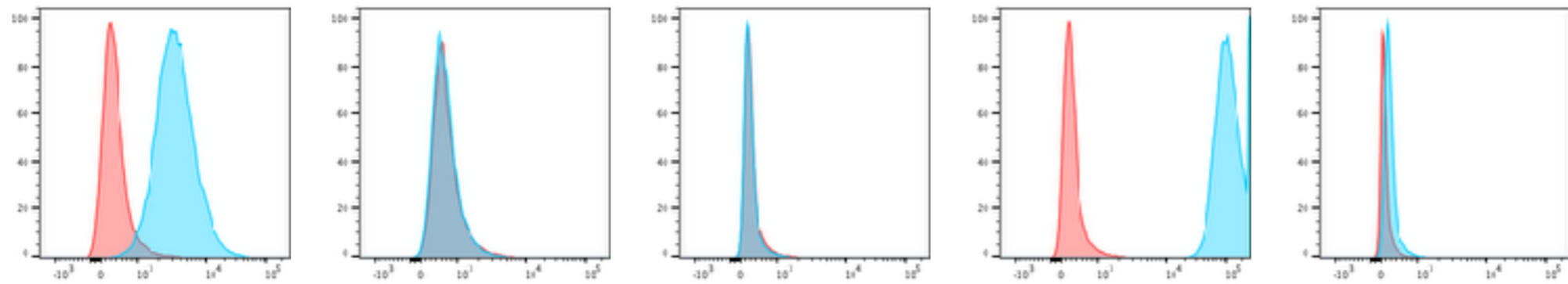
B16



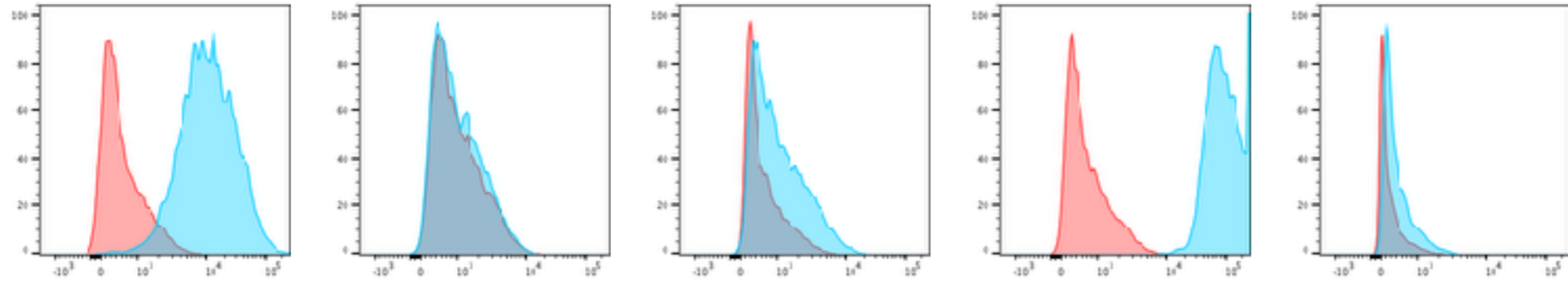
B16-*Pdl1*



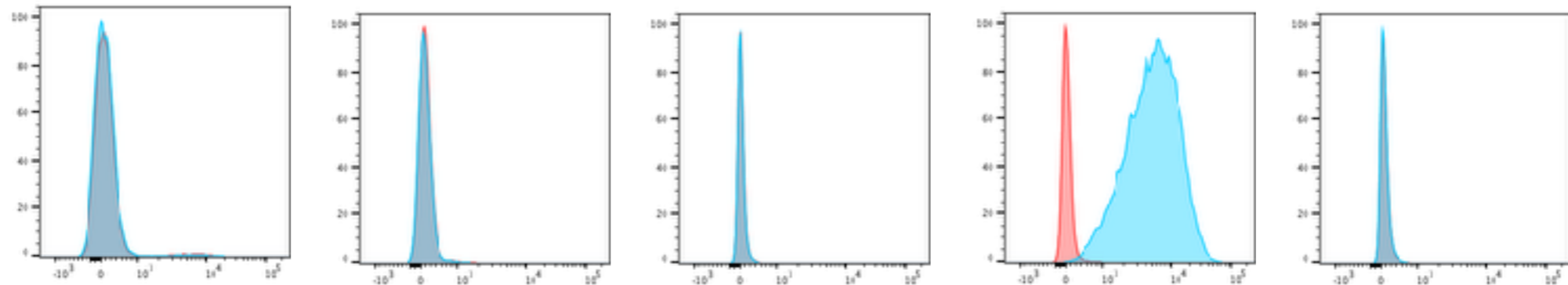
CT26



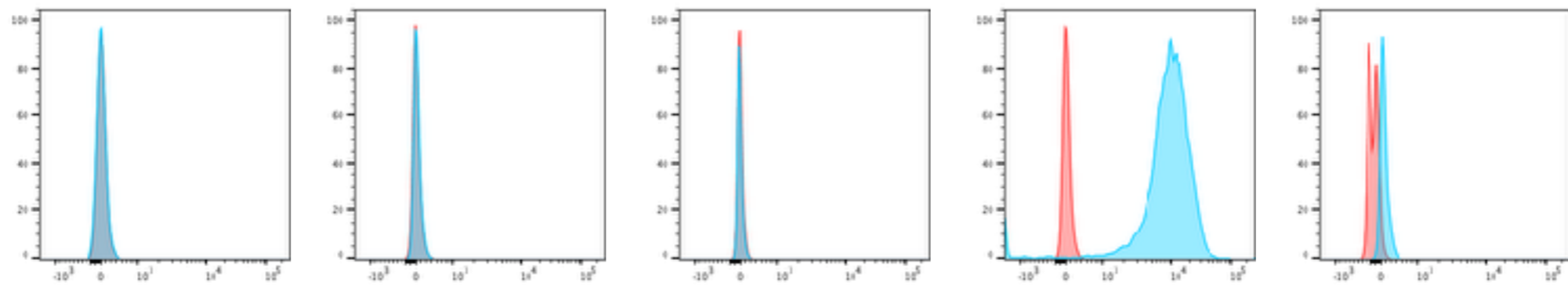
4T1



RMA-S



B16



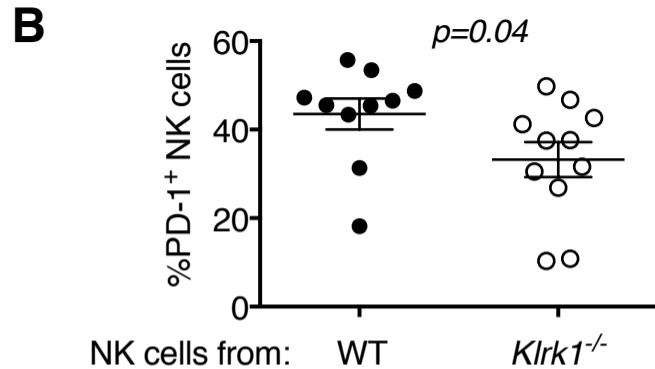
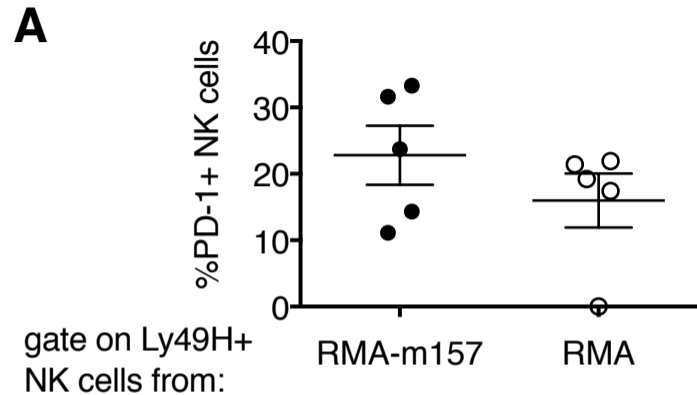
H60

Mult1

Rae1

PVR

Nectin-2



Supplementary Figure 3